JOURNAL OF OPTIMIZATION, DIFFERENTIAL EQUATIONS AND THEIR APPLICATIONS (JODEA)
Volume **31**, Issue **1**, June **2023**, pp. 22–52, DOI 10.15421/142302

ISSN (print) 2617–0108
ISSN (on-line) 2663–6824

SINGULAR DIFFERENTIAL EQUATIONS AND THEIR APPLICATIONS FOR MODELING STRONGLY OSCILLATING PROCESSES

Vasiliy Ye. Belozyorov[*], Svetlana A. Volkova[†], Vadym G. Zaytsev[‡]

Abstract. The normal system of ordinary differential equations, whose right-hand sides are the ratios of linear and nonlinear positive functions, is considered. A feature of these ratios is that some of their denominators can take on arbitrarily small nonzero values. (Thus, the modules of the corresponding derivatives can take arbitrarily large value.) In the sequel, the constructed system of differential equations is used to model strongly oscillating processes (for example, processes determined by the rhythms of electroencephalograms measured at certain points in the cerebral cortex). The obtained results can be used to diagnose human brain diseases.

Key words: system of differential equations, Lyapunov exponents, fractal dimension.

2010 Mathematics Subject Classification: 34A34, 34D20, 37D45, 93A30.

Communicated by Prof. G. Sklyar

1. Introduction

In this article a dynamic process determined by observed electroencephalogram (EEG) rhythms measured at a certain point in the cerebral cortex is investigated [1]– [5]. The main tool of such research is recurrent analysis [6]– [15].

The application of recurrent analysis to the study of EEGs was considered in many scientific articles [2]– [5]. In our opinion, the most fundamental approach to revealing the hidden laws that determine the behavior of the mentioned EEGs was demonstrated in [1].

Let

$$x_0 = x(t_0), x_1 = x(t_1), ..., x_N = x(t_N) \tag{1.1}$$

be a finite sequence (time series) of numerical values of some scalar dynamical variable $x(t)$ measured with the constant time step Δt in the moments $t_i = t_0 + i\Delta t$; $x_i = x(t_i)$; $i = 0, 1, ..., N$ (thus, $\Delta t = t_N/N$) [16–18].

Using the methods of Recurrence Quantification Analysis (RQA), the dimension m of the embedding space and the optimal time delay τ of the mentioned time series are determined.

[*]Department of Applied Mathematics, Oles Honchar Dnipro National University, 72, Gagarin's Avenue, 49010, Dnipro, Ukraine, belozvye2017@gmail.com

[†]Department of Computer Information Technologies, Ukrainian State University of Science and Technologies, Academican Lazaryan's Street, 2, 49010, Dnipro, Ukraine, svolkovav2017@gmail.com

[‡]Department of Applied Mathematics, Oles Honchar Dnipro National University, 72, Gagarin's Avenue, 49010, Dnipro, Ukraine, vadymzaytsev65@gmail.com

It must be said that the quantities m and τ must be determined very precisely. The fact is that if the dimension m is less than the real dimension of the space in which the process takes place, then there is no need to talk about high-quality modeling. With the help of these characteristics, the hidden variables $x(t), y(t), z(t), \ldots$, which determine a system of rational differential equations simulating electrical signals in the cerebral cortex, are restored.

The properties of this system are the main subject of study in this work.

Note that in the problem of studying brain diseases, the time series (1.1) has a chaotic behavior. A common practice in chaotic time series analysis has been to reconstruct the phase space by utilizing the delay-coordinate embedding technique, and then to compute the dynamical invariant magnitudes such as unstable periodic orbits, a fractal dimension of the underlying chaotic set, and its Lyapunov spectrum. As a large body of literature exists on applying of the technique of the time series to study chaotic attractors [19]– [23], a relatively unexplored issue is its applicability to dynamical systems of differential equations depending on parameters. Our focus will be concentrated on the analysis of influence of parameters of found dynamic system on the behavior of its solutions. These parameters are determined by the structure of series (1.1) and by choice of approximating functions in right sides of the got system of differential equations.

To create a model by measuring the variables characterizing any dynamic process, it is necessary to solve the following three main problems.

Usually, a continuous dynamic process is described using a system of differential equations. This remark leads to the first problem.

Problem 1. It is necessary to establish the type of functions on the right side of the differential equations, which most correspond to the description of the processes presented on the electroencephalograms.

It is known that any dynamic process depends on many variables. Most of these variables are functions of some small number of independent variables. Identifying these independent variables leads to the second problem.

Problem 2. Determine the dimension of phase space in which the explored process takes place.

Problem 3. After the structure of the differential equations describing the dynamic process is established, it is necessary to determine the numerical value of coefficients of these equations.

After that, it remains only to check how the resulting model (solutions of the resulting system of differential equations) is adequate to the real process.

2. Mathematical preliminaries

2.1. Model design

We will begin this section by studying **Problem 1**. For this study, we will consider EEGs obtained for healthy and sick patients (see Fig.2.1, Fig.2.2).

Let's note several features inherent in these EEGs.

1. The diagrams have a pronounced oscillating character with a frequency of 400 - 500 hertz.
2. The oscillation amplitudes in the diagram of the sick patient are several times greater than the amplitudes of oscillations in the diagram of the healthy patient.
3. Both diagrams contain a large number of spontaneous bursts of amplitudes, which indicates the chaotic nature of the processes.
4. The presence of times t_i, at which a spontaneous increase in the amplitude of oscillations is observed, indicates that at points t_i there is a sharp increase in the derivative of the process under study; $i = 1, 2, ...$
5. The oscillating process takes place in some ball centered at the point $\mathbf{0}$.

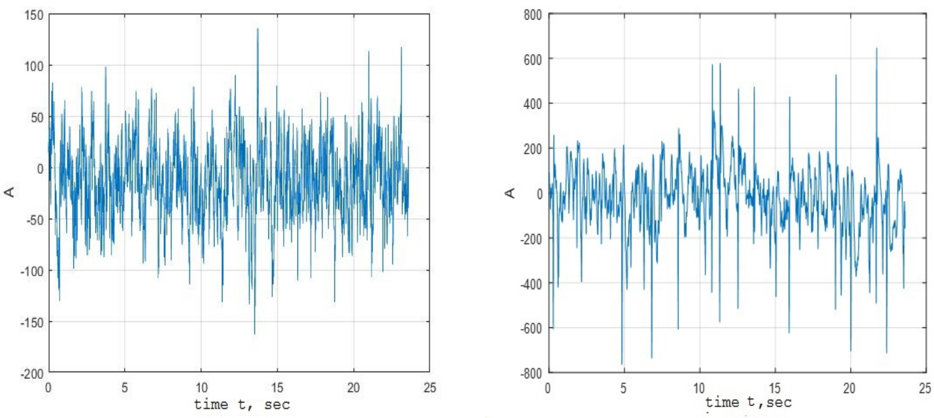

(a1) (a2)

Fig. 2.1. The electroencephalogram taken from a certain point in the cerebral cortex: (a1) a healthy patient, (a2) a patient with an epileptic disease (see [24]).

Let's return to modeling the process $x(t)$, which is generated by the time series (1.1).

We introduce the following real singular function depending on parameters a, b, γ, ω, f and e (or $\delta, \gamma, \beta, \omega, \alpha$ and ε):

$$h(t) = \frac{a \cdot \sin(\gamma t) + b \cdot \cos(\gamma t)}{1 - f \cdot \sin(\omega t) - e \cdot \cos(\omega t)} = \frac{\delta \sin(\gamma t + \beta)}{1 + \varepsilon \cos(\omega t + \alpha)}, \tag{2.1}$$

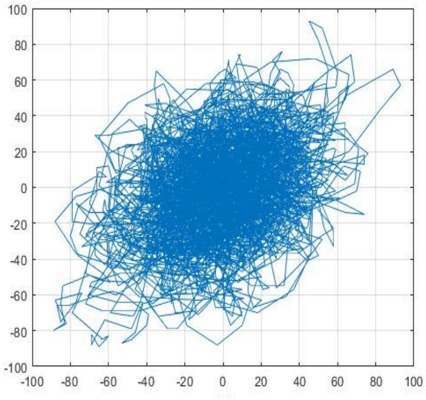

(b1)

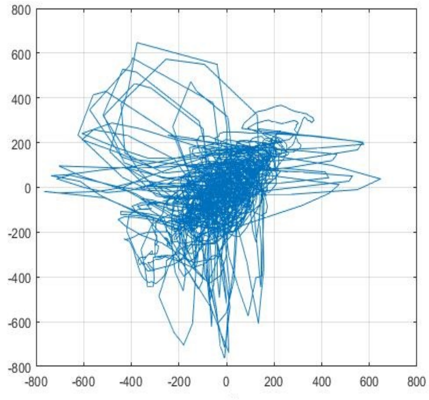

(b2)

Fig. 2.2. Graphs of the same processes as on Fig.2.1, but in coordinates $(x(t), x(t+\tau))$: (b1) the healthy patient, (b2) the patient with an epileptic disease (see [24]).

where $\gamma, \omega \in \mathbb{R}; \delta = \sqrt{a^2+b^2},\ \sin(\beta) = \dfrac{b}{\delta}, \cos(\beta) = \dfrac{a}{\delta};\ |\varepsilon| = \sqrt{f^2+e^2} < 1$, $\sin(\alpha) = \dfrac{f}{\varepsilon}, \cos(\alpha) = -\dfrac{e}{\varepsilon}$ (see Fig.2.3).

Taking into account the form of the function $h(t)$, we can assume that the simplest description of the derivative $\dot{x}(t)$ satisfying items 1) - 5) should look like this:

$$\dot{x}(t) \sim \frac{c \cdot x(t)}{1+\varepsilon\cos(x(t)+\alpha)} + \cdots + \frac{\delta\sin(\omega t+\beta)}{1+\varepsilon\cos(\omega t+\mu)},$$

where the last term takes into account the possibility of the influence of external perturbations on the formation of the structure of differential equations; here $c, \alpha, \varepsilon, \delta, \omega, \beta, \mu$ are real constants.

Using the function $h(t)$, we construct the following system of ordinary differential equations:

$$\begin{cases} \dot{x}_1(t) = \dfrac{a_{11}x_1}{1-f_{11}\sin(x_1)-e_{11}\cos(x_1)} + \dots \\ \qquad + \dfrac{a_{1,n-1}x_{n-1}}{1-f_{1,n-1}\sin(x_{n-1})-e_{1,n-1}\cos(x_{n-1})} \\ \qquad + \dfrac{b_1\sin(x_n)+c_1\cos(x_n)}{1-f_{1n}\sin(x_n)-e_{1n}\cos(x_n)}, \\ \qquad \cdots\cdots\cdots\cdots\cdots\cdots\cdots\cdots\cdots\cdots \\ \dot{x}_{n-1}(t) = \dfrac{a_{n-1,1}x_1}{1-f_{n-1,1}\sin(x_1)-e_{n-1,1}\cos(x_1)} + \dots \\ \qquad + \dfrac{a_{n-1,n-1}x_{n-1}}{1-f_{n-1,n-1}\sin(x_{n-1})-e_{n-1,n-1}\cos(x_{n-1})} \\ \qquad + \dfrac{b_{n-1}\sin(x_n)+c_{n-1}\cos(x_n)}{1-f_{n-1,n}\sin(x_n)-e_{n-1,n}\cos(x_n)}, \\ \dot{x}_n(t) = \omega. \end{cases} \tag{2.2}$$

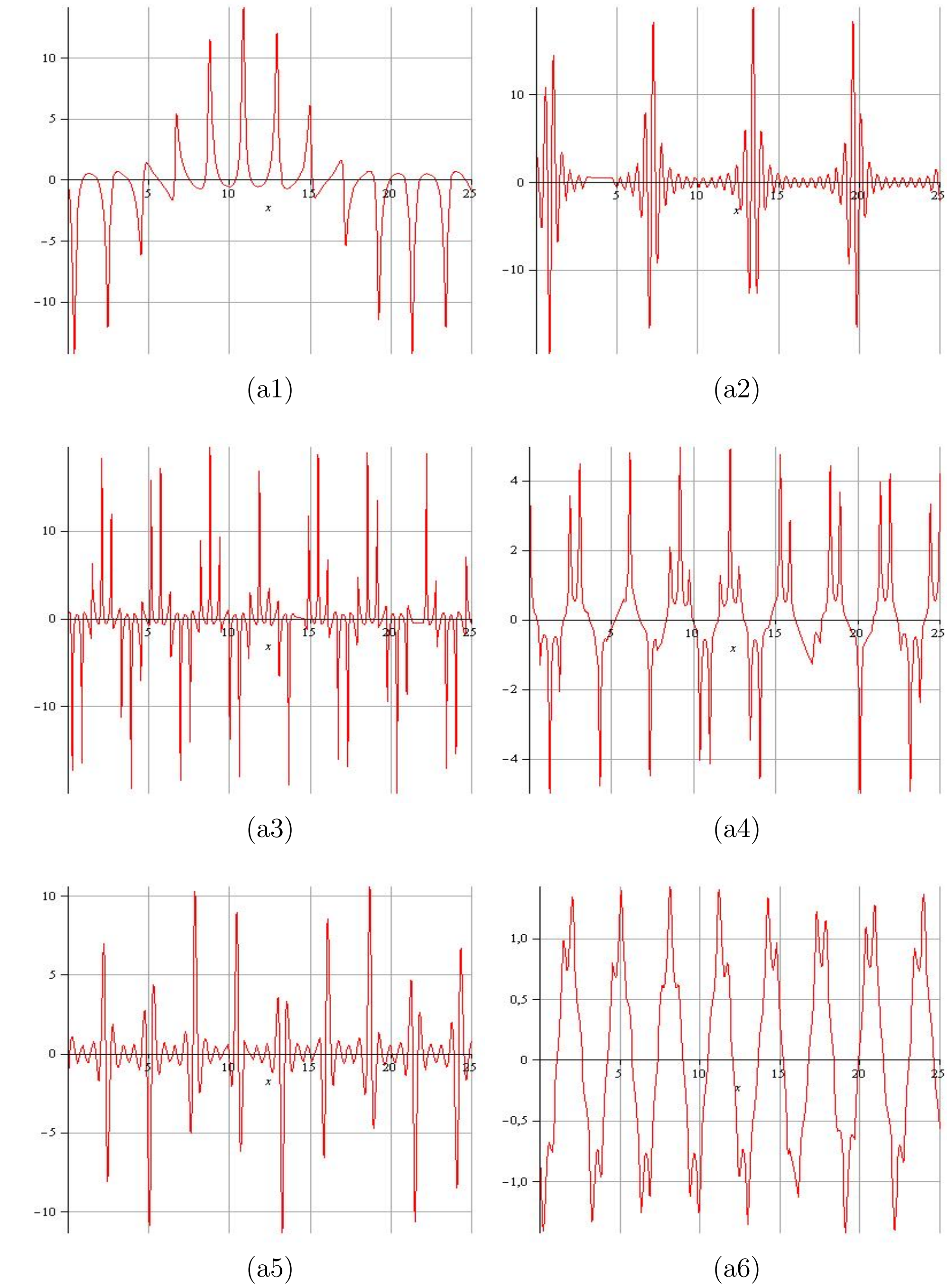

Fig. 2.3. Graphs of function (2.1) for different parameter values: (a1) $\varepsilon = 0.93$, $\gamma = -3.3$, $\beta = 6, \omega = -3, \alpha = -2$; (a2) $\varepsilon = 0.95, \gamma = -12$, $\beta = 2, \omega = 1, \alpha = -4$; (a3) $\varepsilon = 0.95, \gamma = -2$, $\beta = -1, \omega = 10$, $\alpha = 10$; (a4) $\varepsilon = 0.8, \gamma = -10$, $\beta = -10, \omega = -10.3, \alpha = -3$; (a5) $\varepsilon = 0.9, \gamma = 9.9$, $\beta = -1, \omega = 2.3, \alpha = -52$; (a6) $\varepsilon = 0.3, \gamma = -2$, $\beta = -1, \omega = 10, \alpha = 1$; $\delta = 1$.

Here $a_{ij}, f_{ij}, e_{ij}, b_i, c_i, \omega > 0$ are real parameters; $\sqrt{f_{ij}^2 + e_{ij}^2} < 1; i = 1, ..., n - 1; j = 1, ..., n$. (Thus, system (2.2) depends on $(n-1)^2 + 2n(n-1) + 2(n-1) + 1 = n(3n-2)$ parameters, and all of them are rationally included in this system.)

Note that the denominators in the right-hand sides of system (2.2) can take on arbitrarily small positive values.

Definition 2.1. System (2.2) will be called singular.

The inclusion of external perturbations in equations (2.2) cannot always be correctly described. Therefore, sometimes instead of model (2.2), it is necessary to consider the following model

$$\begin{cases} \dot{x}_1(t) = \dfrac{a_{11}x_1}{1 - f_1\sin(x_1) - e_1\cos(x_1)} + \cdots + \dfrac{a_{1,n}x_n}{1 - f_n\sin(x_n) - e_n\cos(x_n)}, \\ \cdots\cdots\cdots\cdots\cdots\cdots\cdots\cdots\cdots\cdots\cdots\cdots\cdots\cdots \\ \dot{x}_n(t) = \dfrac{a_{n,1}x_1}{1 - f_1\sin(x_1) - e_1\cos(x_1)} + \cdots + \dfrac{a_{n,n}x_n}{1 - f_n\sin(x_n) - e_n\cos(x_n)}. \end{cases} \tag{2.3}$$

Now, if we put $\delta = 1, \gamma = 0, \beta = \pi/2$ in formula (2.1), then after a linear change of variables $\mathbf{x} \to A\mathbf{x}$, system (2.3), can be transformed into the following system:

$$\begin{cases} \dot{x}_1(t) = h_1(a_{11}x_1 + \cdots + a_{1n}x_n), \\ \dot{x}_2(t) = h_2(a_{21}x_1 + \cdots + a_{2n}x_n), \\ \quad . \ . \ . \ . \ . \ . \ . \ . \ . \ . \ . \ . \ . \ . \ . \\ \dot{x}_n(t) = h_n(a_{n1}x_1 + \cdots + a_{nn}x_n). \end{cases} \tag{2.4}$$

Here

$$h_i(a_{i1}x_1 + ... + a_{in}x_n) = \frac{a_{i1}x_1 + \cdots + a_{in}x_n}{1 \pm \varepsilon_i \cos(a_{i1}x_1 + \cdots + a_{in}x_n + \alpha_i)},$$

and $\varepsilon_i = \sqrt{f_i^2 + e_i^2} < 1; i = 1, ..., n$.

System (2.4) can be considered as a system of neural ODEs, which makes it possible to use neural network methods for its study [15, 22, 23, 25].

2.2. On boundedness of solutions of singular system (2.2)

We now recall several well-known results from the theory of differential equations [26, 27].

Let's define the norm of the vector $\mathbf{w} = (w_1, ..., w_k)^T \in \mathbb{R}^k$ by the formula $\|\mathbf{w}\| = |w_1| + \cdots + |w_k|$. The norm of matrix $C \in \mathbb{R}^{k\times k}$ is defined similarly: $\|C\| = \sum_{i=1}^k \sum_{j=1}^k |c_{ij}|$.

Consider the system of ordinary differential equations

$$\dot{\mathbf{x}}(t) = (A + B(t))\mathbf{x}(t) + \mathbf{g}(t) \in \mathbb{R}^k, \tag{2.5}$$

where $\mathbf{x}(t) = (x_1(t), ..., x_k(t))^T, \mathbf{g}(t) = (g_1(t), ..., g_k(t))^T \in \mathbb{R}^k, A = \{a_{ij}\}, B(t) = \{b_{ij}(t)\} \in \mathbb{R}^{k\times k}; i, j = 1, ..., k$.

Theorem 2.1. *[26] Assume that for a homogeneous ($\mathbf{g}(t) \equiv \mathbf{0}$) system (2.5) the following conditions are fulfilled:*

(a1) the matrix A is constant and such that its eigenvalues λ_i satisfy the condition $\Re e(\lambda_i) \leq 0, i = 1, ..., k$;

(a2) the variable continuous matrix $B(t)$ depends on time and such that

$$\int_{t_0}^{\infty} \Big\|B(t)\Big\| \, dt < \infty.$$

Then for any vector of initial conditions $\mathbf{x}_0$ the solution $\mathbf{x}(t, \mathbf{x}_0)$ of system (2.5) is bounded at $t \to \infty$.

Theorem 2.2. *[26] Let us assume that under the conditions of Theorem 2.1 for an inhomogeneous ($\mathbf{g}(t) \not\equiv \mathbf{0}$) system (2.5) the following conditions also fulfilled:*

$$\int_{t_0}^{\infty} \operatorname{tr}(A + B(t)) \, dt > -\infty \text{ and } \left\| \int_{t_0}^{\infty} \mathbf{g}(t) \, dt \right\| < \infty.$$

Then for any vector of initial conditions $\mathbf{x}_0$ the solution $\mathbf{x}(t, \mathbf{x}_0)$ of system (2.5) is bounded at $t \to \infty$.

Theorem 2.3. *[26] If the function $\phi(t)$ tends monotonically to zero ($\lim_{t\to\infty} \phi(t) = 0$) and the function $\psi(t)$ has a bounded antiderivative ($\int_{t_0}^{\infty} \psi(t) \, dt < \infty$), then the integral $\int_{t_0}^{\infty} \phi(t)\psi(t) \, dt$ converges.*

Theorem 2.4. *[27] (Global Existence and Uniqueness) Suppose that the function $\mathbf{F}(t, \mathbf{x}) \in \mathbb{R}^k$ is piecewise continuous in t and $\forall \mathbf{x}, \mathbf{y} \in \mathbb{R}^k, \forall t \in [t_0, \infty)$ satisfies the conditions*

$$\|\mathbf{F}(t, \mathbf{x}) - \mathbf{F}(t, \mathbf{y})\| \leq L\|\mathbf{x} - \mathbf{y}\| \text{ and } \|\mathbf{F}(t, \mathbf{x}_0)\| \leq P,$$

where $L > 0, P > 0$ are constants. Then, the state equation $\dot{\mathbf{x}}(t) = \mathbf{F}(t, \mathbf{x})$ with the initial condition $\mathbf{x}(t_0) = \mathbf{x}_0$ has a unique solution over $[t_0, \infty)$.

Let $\mathbf{x}_1 = (x_1, ..., x_{n-1})^T \in \mathbb{R}^{n-1}$. We introduce the following square matrices

$$A_1 = \{a_{ij}\}, \ B_1(\mathbf{x}_1) = \left\{ a_{ij} \frac{f_{ij} \sin(x_j) + e_{ij} \cos(x_j)}{1 - f_{ij} \sin(x_j) - e_{ij} \cos(x_j)} \right\} \in \mathbb{R}^{(n-1)\times(n-1)};$$

$i, j = 1, ..., n - 1$.

Let us also introduce the real $(n - 1)$-vector

$$\mathbf{g}_1(t) = \left(\frac{b_1 \sin(\omega t) + c_1 \cos(\omega t)}{1 - f_{1,n} \sin(\omega t) - e_{1,n} \cos(\omega t)}, ..., \frac{b_{n-1} \sin(\omega t) + c_{n-1} \cos(\omega t)}{1 - f_{n-1,n} \sin(\omega t) - e_{n-1,n} \cos(\omega t)} \right)^T.$$

In this case, instead of system (2.2), we can consider the following system

$$\dot{\mathbf{x}}_1(t) = (A_1 + B_1(\mathbf{x}_1))\mathbf{x}_1 + \mathbf{g}_1(t) \in \mathbb{R}^{n-1} \tag{2.6}$$

with the initial condition $\mathbf{x}_1(t_0) = \mathbf{x}_{10}$.

The following theorem is the main one in this paper.

Theorem 2.5. *Let the matrix* $A_1 = \{a_{ij}\}; i, j = 1, ..., n-1$, *in singular system (2.6) be Hurwitz. If* $\sqrt{f_{ij}^2 + e_{ij}^2} < 1; i = 1, ..., n-1; j = 1, ..., n$, *then for any vector of initial conditions* $\mathbf{x}_{10}$ *the solution* $\mathbf{x}_1(t, \mathbf{x}_{10})$ *of system (2.6) is bounded at* $t \to \infty$.

Proof. (c1) Let us estimate the norm of the matrix $(A_1 + B_1(\mathbf{x}_1))$. Since $\sqrt{f_{ij}^2 + e_{ij}^2} < 1$, then we have

$$\begin{aligned}\|A_1 + B_1(\mathbf{x}_1)\| &= \sum_{i=1}^{n-1}\sum_{j=1}^{n-1} \frac{|a_{ij}|}{1 - f_{ij}\sin(x_j) - e_{ij}\cos(x_j)} \\ &\le \sum_{i=1}^{n-1}\sum_{j=1}^{n-1} \frac{|a_{ij}|}{1 - \sqrt{f_{ij}^2 + e_{ij}^2}} = K > 0.\end{aligned}$$

(c2) Let $\mathbf{g}_1(t) \equiv 0$. Now suppose that a solution $\mathbf{w}(t) = \mathbf{x}_1(t, \mathbf{x}_{10})$ of system (2.6) exists. Then we can estimate its norm $\|\mathbf{w}(t)\|$.

We have

$$\mathbf{w}(t) = \exp(A_1 t_0)\mathbf{w}(t_0) + \int_{t_0}^{\infty} \exp(A_1(t-\tau))B_1(\mathbf{w}(\tau))\mathbf{w}(\tau)\, d\tau$$

and

$$\|\mathbf{w}(t)\| \le \|\exp(A_1 t_0)\|\|\mathbf{w}(t_0)\| + \int_{t_0}^{\infty} \|\exp(A_1(t-\tau))B_1(\mathbf{w}(\tau))\|\|\mathbf{w}(\tau)\|\, d\tau$$

Since the matrix A_1 is Hurwitz, then we have $\|\exp(A_1 t)\| < c \cdot \exp(-\Lambda t) < c \cdot \exp(-\Lambda t_0) = N_1$ and according to the Bellman-Gronwall Lemma [27], we have

$$\|\mathbf{w}(t)\| \le N_1 \|\mathbf{w}(t_0)\| \exp\Big(\int_{t_0}^{\infty} \|\exp(A_1(\tau)B_1(\mathbf{w}(\tau))\|\, d\tau\Big), \tag{2.7}$$

where $c > 0$, $-\Lambda = \max(\Re e(\lambda_1), ..., \Re e(\lambda_n)) < 0$, and $\lambda_1, ..., \lambda_n$ are eigenvalues of matrix A_1.

A rougher estimate of the norm $\|\mathbf{w}(t)\|$ can be obtained as follows:

$$\|\dot{\mathbf{w}}(t)\| \le \|A_1 + B_1(\mathbf{w}_1(t))\| \cdot \|\mathbf{w}(t)\| \le K\|\mathbf{w}(t)\|.$$

From here it follows that $\|\mathbf{w}(t)\| \le \exp(Kt)\|\mathbf{w}(t_0)\|$.

(c3) Now, let's estimate the integral

$$\int_{t_0}^{\infty} \exp(A_1(\tau)B_1(\mathbf{w}(\tau))\, d\tau, \tag{2.8}$$

where the elements of the matrix B_1 are

$$b_{ij} = a_{ij}\frac{f_{ij}\sin(w_j(t)) + e_{ij}\cos(w_j(t))}{1 - f_{ij}\sin(w_j(t)) - e_{ij}\cos(w_j(t))}.$$

Let t_k be the root of the equation $w_j(t_{j,k+1}) = w_j(t_{j,k}) + 2\pi; j = 1, ..., n-1; k = 0, 1, ...$ In this case, we can get the following estimate:

$$\left\| \int_{t_0}^{\infty} \exp(A_1(\tau) B_1(\mathbf{w}(\tau))\, d\tau \right\| \leq \int_{t_0}^{\infty} \left\| \exp(A_1(\tau) B_1(\mathbf{w}(\tau)) \right\| d\tau$$
$$\leq \sum_{i=1}^{n-1} \sum_{j=1}^{n-1} \frac{c|a_{ij}|}{1 - \sqrt{f_{ij}^2 + e_{ij}^2}}$$
$$\times \left[\lim_{l\to\infty} \underbrace{\sum_{k=0}^{l} \int_{t_{j,k}}^{t_{j,k+1}} \exp(-\Lambda t) |f_{ij} \sin(w_j(t)) + e_{ij} \cos(w_j(t))|\, dt}_{\hookrightarrow 0} \right.$$
$$\left. + \int_{t_{j,l+1}}^{t_{j,\xi(l)}} \exp(-\Lambda t) |f_{ij} \sin(w_j(t)) + e_{ij} \cos(w_j(t))|\, dt \right]$$
$$\leq \sum_{i=1}^{n-1} \sum_{j=1}^{n-1} \frac{c|a_{ij}|}{1 - \sqrt{f_{ij}^2 + e_{ij}^2}} \int_{t_{j,l+1}}^{t_{j,\xi(l)}} \exp(-\Lambda t) |f_{ij} \sin(w_j(t)) + e_{ij} \cos(w_j(t))|\, dt$$
$$\leq 2c_0 \sum_{i=1}^{n-1} \sum_{j=1}^{n-1} \frac{|a_{ij}| \sqrt{f_{ij}^2 + e_{ij}^2}}{1 - \sqrt{f_{ij}^2 + e_{ij}^2}} \int_{t_{j,l+1}}^{t_{j,\xi(l)}} |\sin(w_j(t)) + \cos(w_j(t))|\, dt$$
$$\leq 2c_0 \sum_{i=1}^{n-1} \sum_{j=1}^{n-1} \frac{|a_{ij}| \sqrt{f_{ij}^2 + e_{ij}^2}}{1 - \sqrt{f_{ij}^2 + e_{ij}^2}} < \infty.$$

Here $c_0 = c \cdot (\Lambda)^{-1} \cdot \exp(-\Lambda t_0); w_j(t_{j,\xi(l)}) < w_j(t_{j,l+1}) + 2\pi; j = 1, ..., n-1.$

Thus, integral (2.8) is bounded.

As follows from item (c2), the solution $\mathbf{w}(t)$ of system (2.6) has an order of growth no higher than the function $\exp(N_1 t)$:

$$\lim_{t\to\infty} \frac{\|\mathbf{w}(t)\|}{\exp(Kt)} = l \ (0 \leq l < \infty). \tag{2.9}$$

Taking into account (2.9) ($\|\mathbf{w}(t)\| \sim l \exp(Kt)$), we estimate the integral

$$H_{ij} = \int_{t_0}^{\infty} \frac{f_{ij} \sin(w_j(t)) + e_{ij} \cos(w_j(t))}{1 - f_{ij} \sin(w_j(t)) - e_{ij} \cos(w_j(t))}\, dt.$$

Since $\varepsilon_{ij} = \sqrt{f_{ij}^2 + e_{ij}^2} < 1$, it is obvious that

$$H_{ij} \sim Q_{ij} = \int_{t_0}^{\infty} \frac{f_{ij} \sin(l \exp(Kt)) + e_{ij} \cos(l \exp(Kt))}{1 - f_{ij} \sin(l \exp(Kt)) - e_{ij} \cos(l \exp(Kt))}\, dt.$$

Let's change the variable $s(t) = l \exp(N_1 t)$. Then we will have

$$H_{ij} \sim Q_{ij} = \int_{s_0}^{\infty} \frac{\delta_{ij} \sin(s + \beta_{ij})}{s(1 + \varepsilon_{ij} \cos(s + \alpha_{ij}))}\, ds = \int_{s_0}^{\infty} \frac{h_{ij}(s)\, ds}{s},$$

where the function $h_{ij}(s)$ is defined by formula (2.1) and $s_0 = s(t_0) = l\exp(Kt_0)$.

The improper integral Q_{ij} can be written as follows

$$Q_{ij} = \int_{s_0}^{\infty} \phi(s)\psi(s)\,ds,$$

where the functions $\phi(s)$ and $\psi(s)$ satisfy the conditions

$$\lim_{s\to\infty}\phi(s) = \lim_{s\to\infty}\frac{1}{s} = 0,\ \lim_{s\to\infty}\int_{s_0}^{\infty}\psi(s)\,ds = \lim_{s\to\infty}\int_{s_0}^{s}\frac{\delta_{ij}\sin(s+\beta_{ij})}{1+\varepsilon_{ij}\cos(s+\alpha_{ij})}\,ds$$
$$\le \lim_{s\to\infty}\frac{|\delta_{ij}|}{\sqrt{1-\varepsilon_{ij}^2}}\left|\int_{s_0}^{s}\sin(s+\beta_{ij})\,ds\right| \le \frac{2|\delta_{ij}|}{\sqrt{1-\varepsilon_{ij}^2}} < \infty.$$

Thus, the indicated functions $\phi(s)$ and $\psi(s)$ satisfy the conditions of Theorem 2.3. Consequently, the integral Q_{ij} and also the integral H_{ij} converge. Therefore, integral (2.8) also converges. Then according to (2.7), we get $\|\mathbf{w}(t)\| < \infty$. All conditions of Theorem 2.1 are satisfied.

(c4) Now let $\mathbf{g}_1(t) \not\equiv 0$. It is necessary to estimate the integral

$$\int_{t_0}^{\infty}\mathbf{g}_1(t)\,dt.$$

Any component of the vector $\mathbf{g}_1(t)$ has the form

$$g_{in} = \frac{b_i\sin(\omega t) + c_i\cos(\omega t)}{1 - f_{in}\sin(\omega t) - e_{in}\cos(\omega t)}.$$

Further reasoning repeats the reasoning of item (c3).

Let us introduce a number $t_{i,k}$ such that $\omega t_{i,k+1} = \omega t_{i,k} + 2\pi$. In this case, we can get the following estimate:

$$\left\|\int_{t_0}^{\infty}\mathbf{g}_1(t)\,dt\right\| = \sum_{i=1}^{n-1}\left|\int_{t_0}^{\infty}g_{in}(t)\,dt\right| \le \sum_{i=1}^{n-1}\frac{1}{\sqrt{1-\varepsilon_{in}^2}}$$
$$\times\Bigg[\lim_{l\to\infty}\sum_{k=0}^{l}\underbrace{\left|\int_{t_{i,k}}^{t_{i,k+1}}(b_i\sin(\omega t)+c_i\cos(\omega t))\,dt\right|}_{\hookrightarrow 0}$$
$$+\left|\int_{t_{i,l+1}}^{t_{i,\xi(l)}}(b_i\sin(\omega t)+c_i\cos(\omega t))\,dt\right|\Bigg]$$
$$\le \sum_{i=1}^{n-1}\frac{\sqrt{b_i^2+c_i^2}}{\sqrt{1-\varepsilon_{in}^2}}\times\Bigg[\lim_{l\to\infty}\sum_{k=0}^{l}\underbrace{\left|\int_{t_{i,k}}^{t_{i,k+1}}(\sin(\omega t)+\cos(\omega t))\,dt\right|}_{\hookrightarrow 0}$$
$$+\left|\int_{t_{i,l+1}}^{t_{i,\xi(l)}}(\sin(\omega t)+\cos(\omega t))\,dt\right|\Bigg] \le 2\sum_{i=1}^{n-1}\frac{\sqrt{b_i^2+c_i^2}}{\sqrt{1-\varepsilon_{in}^2}} = N_2 < \infty,$$

where $N_2 > 0$ is a constant.

Further, using the technique of proving that the integral H_{ij} is bounded (see item (c3)) and condition $a_{11} + \cdots + a_{nn} < 0$ (see [26]), we obtain

$$\int_{t_0}^{\infty} \operatorname{tr}(A_1 + B_1(\mathbf{w}_1(t))\, dt = \sum_{i=1}^{n-1} \int_{t_0}^{\infty} \frac{a_{ii}}{1 - f_{ii}\sin(w_i(t)) - e_{ii}\cos(w_i(t))}\, dt$$
$$= \sum_{i=1}^{n-1} a_{ii} \int_{s_0}^{\infty} \frac{ds}{s(1 + \varepsilon_{ii}\cos(s + \alpha_{ii}))}. \tag{2.10}$$

For the integral in formula (2.10), we have the following estimate:

$$\lim_{s\to\infty} \int_{s_0}^{s} \frac{ds}{1 + \varepsilon_{ii}\cos(s + \alpha_{ii})}$$
$$= \lim_{s\to\infty} \frac{2}{\sqrt{1-\varepsilon_{ii}^2}} \arctan\left(\sqrt{\frac{1-\varepsilon_{ii}}{1+\varepsilon_{ii}}} \tan\frac{s+\alpha_{ii}}{2}\right)$$
$$- \frac{2}{\sqrt{1-\varepsilon_{ii}^2}} \arctan\left(\sqrt{\frac{1-\varepsilon_{ii}}{1+\varepsilon_{ii}}} \tan\frac{s_0+\alpha_{ii}}{2}\right) < \frac{2\pi}{\sqrt{1-\varepsilon_{ii}^2}}.$$

Now the last inequality and Theorem 2.3 allow us to obtain such an estimate for integral (4.2):

$$\int_{t_0}^{\infty} \operatorname{tr}(A_1 + B_1(\mathbf{w}_1(t))\, dt > 2\pi(a_{11} + \cdots + a_{n-1,n-1}) \sum_{i=1}^{n-1} \frac{1}{\sqrt{1-\varepsilon_{ii}^2}} > -\infty.$$

Now, to prove the boundedness of the solutions of system (2.6), it only remains to apply Theorem 2.2.

(c5) Consider the linear system

$$\dot{\mathbf{x}}_1(t) = (A_1 + B_1(\mathbf{w}(t)))\mathbf{x}_1 + \mathbf{g}_1(t) \in \mathbb{R}^{n-1}. \tag{2.11}$$

where $B_1(\mathbf{w}(t))$ is piecewise continuous functions of t.

Now we check the fulfillment of the conditions of Theorem 2.4 for system (2.6). Over any finite interval of time $[t_0, \infty)$, the elements of $A_1 + B_1(\mathbf{w}(t))$ are bounded. Therefore, we have

$$\|\mathbf{F}(t, \mathbf{x}_1) - \mathbf{F}(t, \mathbf{y}_1)\| = \|(A_1 + B_1(\mathbf{x}_1))\mathbf{x}_1 - (A_1 + B_1(\mathbf{y}_1))\mathbf{y}_1\| \le N_1\|\mathbf{x}_1 - \mathbf{y}_1\|,$$

$$\|\mathbf{F}(t, \mathbf{x}_{10})\| = \|(A_1 + B_1(\mathbf{x}_{10}))\mathbf{x}_{10} + \mathbf{g}_1(t)\| \le N_1\|\mathbf{x}_{10}\| + N_2 \le P.$$

Thus, if $L = N_1$, $P > N_2$, and $\|\mathbf{x}_{10}\| \le (P - N_2)/N_1$, then the conditions of Theorem 2.4 are satisfied for any $t \in [t_0, \infty)$. This means that under these conditions a solution to system (2.6) exists and is unique.

The proof of Theorem 2.5 is complete. $\square$

Note that systems (2.3) and (2.4) are particular cases of system (2.6) (Only it should be remembered that in these systems $A \in \mathbb{R}^{n\times n}$.) Therefore, Theorem 2.5 is also true for systems (2.3) and (2.4).

3. Rationale for using equations (2.2) to model EEG rhythms

In the study of dynamic processes, as a rule, only a few variables describing the process are available for direct measurement. The remaining variables (the so-called hidden variables) are inaccessible to observation. This raises the problem of reconstructing these unobserved variables from known observable variables. The first step towards solving this problem is to establish the minimum number of all variables (measured and hidden) on which the dynamic process depends (**Problem 2**).

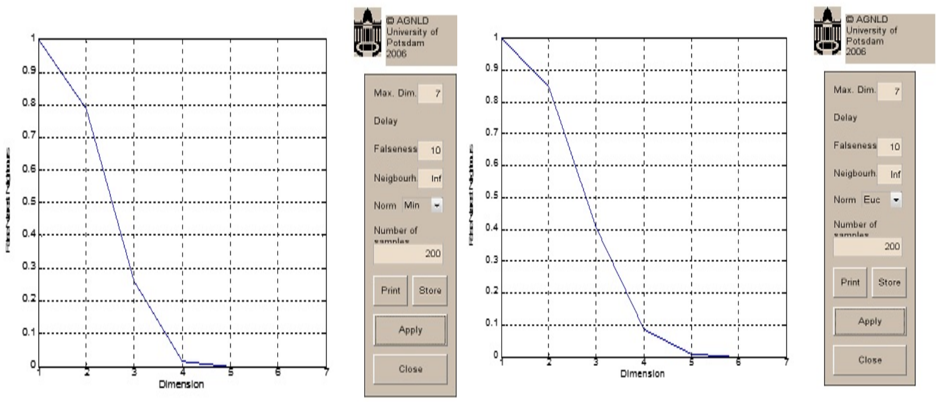

(a1) (a2)

Fig. 3.1. Dimension of the embedding space for time series (1.1): healthy (a1) and sick (a2) patients.

Consider the time series (1.1). Using the recurrent analysis [2, 17, 18, 25, 28], we calculate the dimension m of the embedding space and the optimal time delay τ. Using these characteristics, we construct m time series

$$\left\{\begin{array}{ll} x_1(t) = \{x_1(t_0) = x(t_0), & x_2(t) = \{x_2(t_0) = x(t_0+\tau), \\ \quad x_1(t_1) = x(t_1), & \quad x_2(t_1) = x(t_1+\tau), \\ \quad \vdots & \quad \vdots \\ \quad x_1(t_k) = x(t_k)\}, & \quad x_2(t_k) = x(t_k+\tau)\}, \\ \multicolumn{2}{c}{\dots\dots\dots\dots\dots\dots} \\ \multicolumn{2}{c}{x_m(t) = \{x_m(t_0) = x(t_0+(m-1)\tau),} \\ \multicolumn{2}{c}{\quad x_m(t_1) = x(t_1+(m-1)\tau),} \\ \multicolumn{2}{c}{\vdots} \\ \multicolumn{2}{c}{\quad x_m(t_k) = x(t_k+(m-1)\tau)\},} \end{array}\right. \tag{3.1}$$

defining the behavior of a real dynamical system. (Here $t_k + (m-1)\tau < t_N$.)

As experimental studies show, the processes presented in Fig.2.1 can be embedded in the phase space, the dimension of which is $4, 5$, or 6 [28]. Therefore, in the future, we will assume that $m = 5$ (see Fig.3.1).

In addition, at the next stage of modeling (see Section 4), a model will be built that depends on a small number of parameters and adequately describes the processes presented in Fig.2.1.

In the case $m = 5$, to simplify system (2.2), some of the parameters f_{ij}, e_{ij} in the denominators will be omitted. As a result, instead of $(m-1)^2 + 2m(m-1) + 2(m-1) + 1 = 16 + 40 + 8 + 1 = 65$ parameters, the newly obtained system will contain only 16+10+8+1=35 parameters $a_{ij}, f_i, e_i, b_i, c_i, \omega$. An example of such system is given below:

$$\begin{cases} \dot{x}(t) = \dfrac{0 \cdot x}{1 - 0.23\sin(x) + 0.85\cos(x)} + \dfrac{1 \cdot y}{1 + 0.72\sin(y) - 0.37\cos(y)} \\ \quad + \dfrac{-10.1 \cdot z}{1 - 0.67\sin(z) + 0.67\cos(z)} + \dfrac{0 \cdot u}{1 + 0.68\sin(u) - 0.68\cos(u)} \\ \quad + \dfrac{0 \cdot \sin(v) + 0 \cdot \cos(v)}{1 - 0.69\sin(v) + 0.70\cos(v)}, \\ \dot{y}(t) = \dfrac{-11 \cdot x}{1 - 0.23\sin(x) + 0.85\cos(x)} + \dfrac{-0.1 \cdot y}{1 + 0.72\sin(y) - 0.37\cos(y)} \\ \quad + \dfrac{0 \cdot z}{1 - 0.67\sin(z) + 0.67\cos(z)} + \dfrac{10.9 \cdot u}{1 + 0.68\sin(u) - 0.68\cos(u)} \\ \quad + \dfrac{0 \cdot \sin(v) + 0 \cdot \cos(v)}{1 - 0.69\sin(v) + 0.70\cos(v)}, \\ \dot{z}(t) = \dfrac{10 \cdot x}{1 - 0.23\sin(x) + 0.85\cos(x)} + \dfrac{0 \cdot y}{1 + 0.72\sin(y) - 0.37\cos(y)} \\ \quad + \dfrac{0 \cdot z}{1 - 0.67\sin(z) + 0.67\cos(z)} + \dfrac{1 \cdot u}{1 + 0.68\sin(u) - 0.68\cos(u)} \\ \quad + \dfrac{0 \cdot \sin(v) + 110 \cdot \cos(v)}{1 - 0.69\sin(v) + 0.70\cos(v)}, \\ \dot{u}(t) = \dfrac{0 \cdot x}{1 - 0.23\sin(x) + 0.85\cos(x)} + \dfrac{-20 \cdot y}{1 + 0.72\sin(y) - 0.37\cos(y)} \\ \quad + \dfrac{-110.4 \cdot z}{1 - 0.67\sin(z) + 0.67\cos(z)} + \dfrac{-0.1 \cdot u}{1 + 0.68\sin(u) - 0.68\cos(u)} \\ \quad + \dfrac{-100 \cdot \sin(v) - 110 \cdot \cos(v)}{1 - 0.69\sin(v) + 0.70\cos(v)}, \\ \dot{v}(t) = \omega. \end{cases} \tag{3.2}$$

The following Fig.3.2 shows the application of system (3.2) (at certain values of the coefficients) for modeling the processes shown in Fig.2.1.

Thus, model (3.2), with the help of appropriate parameter settings, can correctly describe the dynamics of rhythms (see Fig.3.2) in the cerebral cortex, shown in Fig.2.1.

In the case of $m = 5$, system (3.2) can be transformed into system (2.3). For this, it is necessary:

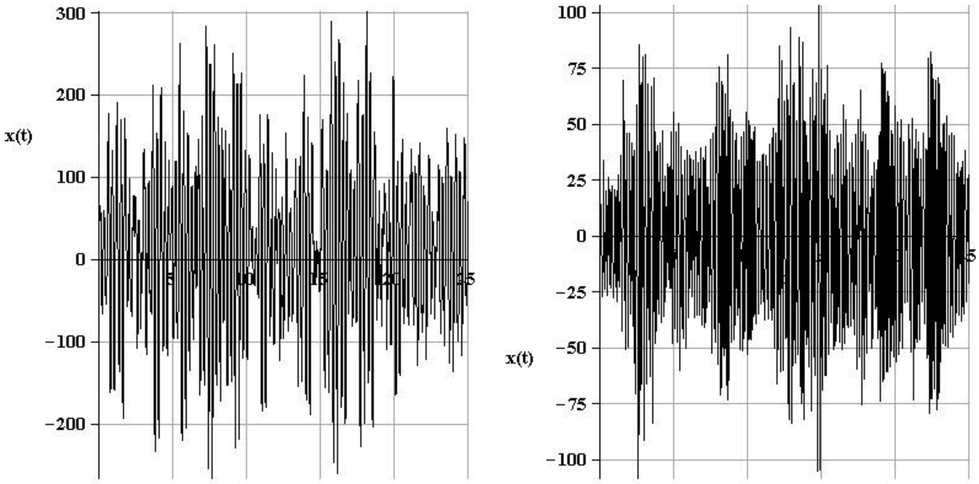

(a1) (a2)

Fig. 3.2. Simulation of the process shown in Fig.2.1 with the help of system (3.2): (a1) $\omega = 10.5$; (a2) $\omega = 12$.

1) In the first four equations of system (3.2), make substitutions $b_i \sin(v) + c_i \cos(v) \to a_{i5}v; i = 1, ..., 4$;

2) Replace the fifth equation of system system (3.2) with equation

$$
\begin{aligned}
\dot{v}(t) = & \frac{a_{51}x}{1 - f_1 \sin(x) - e_1 \cos(x)} + \frac{a_{52}y}{1 - f_2 \sin(y) - e_2 \cos(y)} \\
& + \frac{a_{53}z}{1 - f_3 \sin(z) - e_3 \cos(z)} + \frac{a_{54}u}{1 - f_4 \sin(u) - e_4 \cos(u)} \\
& + \frac{a_{55}v}{1 - f_5 \sin(v) - e_5 \cos(v)}.
\end{aligned}
$$

Note that the number of parameters in the newly obtained system at $m = 5$ will remain the same: 35.

4. Simplified identification of processes described by system (2.2)

In this section, we will begin to solve **Problem 3**. In the future, the number of variables in systems of equations, we will denote by n, where $n \geq m = 5$.

Note that the bounded variables $x_2(t), ..., x_n(t)$ derived from the measured variable $x_1(t) = x(t)$. Therefore, for models built using EEG, the equation $\dot{x}_n(t) = \omega$ must be replaced by the equation $\dot{x}_n(t) = a_{nn}x_n(t) + \phi(x_1(t), ..., x_{n-1}(t))$, where $a_{nn} < 0$. A possible form of such model can be as follows:

$$\begin{cases} \dot{x}_1(t) &= \dfrac{a_{10} + \cdots + a_{1,n-1}x_{n-1} + b_1\sin(x_n) + c_1\cos(x_n)}{1 - f_1\sin(x_n) - e_1\cos(x_n)}, \\ &= \ldots\ldots\ldots\ldots\ldots\ldots\ldots\ldots\ldots\ldots\ldots\ldots \\ \dot{x}_{n-1}(t) &= \dfrac{a_{n-1,0} + \cdots + a_{n-1,n-1}x_{n-1} + b_{n-1}\sin(x_n) + c_{n-1}\cos(x_n)}{1 - f_{n-1}\sin(x_n) - e_{n-1}\cos(x_n)}, \\ \dot{x}_n(t) &= \omega_0 + \omega_1 x_1 + \cdots + \omega_n x_n. \end{cases} \tag{4.1}$$

Here $a_{ij}, f_i, e_i, b_i, c_i, \omega_i$ are real parameters; $\sqrt{f_i^2 + e_i^2} < 1; i = 1, ..., n-1; j = 0, ..., n$. (Thus, system (4.1) depends on $(n-1)n + 4(n-1) + n + 1 = n^2 + 4n - 3$ parameters, and all of them are rationally included in this system.)

Note that by replacing

$$x_n(t) = \omega_0 t + \int_{t_0}^{t} (\omega_1 x_1(t) + \cdots + \omega_n x_n(t))\, dt \to \omega t,$$

system (4.1) can be reduced to system (2.6) . This means that under the conditions of Theorem 2.5 the solutions of system (4.1) will be bounded. (To prove Theorem 2.5 for system (4.1), it is necessary to slightly change item (c4) in its proof. In the presence of item (c3) in the same proof, such changes are quite obvious.)

Model (4.1) is still difficult to study. Therefore, in the future we will focus on the study of the following model:

$$\begin{cases} \dot{x}_1(t) = \dfrac{1}{1 - f_1\sin(x_i) - e_1\cos(x_i)} \displaystyle\sum_{j=0, j\neq i}^{n} a_{1j}x_j, \\ \cdot\ , \\ \dot{x}_i(t) = \dfrac{1}{1 - f_i\sin(x_i) - e_i\cos(x_i)} \displaystyle\sum_{j=0}^{n} a_{ij}x_j, \\ \cdot\ , \\ \dot{x}_n(t) = \dfrac{1}{1 - f_n\sin(x_i) - e_n\cos(x_i)} \displaystyle\sum_{j=0, j\neq i}^{n} a_{nj}x_j. \end{cases} \tag{4.2}$$

Here $f_i^2 + e_i^2 < 1; i \in \{1, ..., n\}$. (In total, n different models of type (4.2) can be designed in this way.)

Let us introduce the following matrix

$$A_i = \begin{pmatrix} a_{11} & \cdots & a_{1,i-1} & a_{1,i+1} & \cdots & a_{1n} \\ \vdots & \ddots & \vdots & \vdots & \vdots & \vdots \\ a_{i-1,1} & \cdots & a_{i-1,i-1} & a_{i-1,i+1} & \cdots & a_{i-1,n} \\ a_{i+1,1} & \cdots & a_{i+1,i-1} & a_{i+1,i+1} & \cdots & a_{+1,n} \\ \vdots & \vdots & \vdots & \vdots & \ddots & \vdots \\ a_{n1} & \cdots & a_{n,i-1} & a_{n,i+1} & \cdots & a_{nn} \end{pmatrix} \in \mathbb{R}^{(n-1)\times(n-1)}.$$

Theorem 4.1. *Suppose that for some $i \in \{1, ..., n\}$ the matrix A_i for the singular system (4.2) be Hurwitz. If $\forall i \in \{1, ..., n\}$, we have $\sqrt{f_i^2 + e_i^2} < 1$, then for any vector of initial conditions $\mathbf{x}_0$ the solutions*

$$x_1(\mathbf{x}_0)(t), ..., x_{i-1}(\mathbf{x}_0)(t), x_{i+1}(\mathbf{x}_0)(t), ..., x_n(\mathbf{x}_0)(t)$$

of system (4.2) is bounded at $t \to \infty$. If, in addition, $a_{ii} < 0$, then the solution $x_i(\mathbf{x}_0)(t)$ is also bounded.

Proof. Let the vector $\mathbf{b} = (b_1, ..., b_i, b_{i+1}, ..., b_n)^T$ be the solution of the linear equation $\mathbf{a} + A_i\mathbf{b} = 0$, where $\mathbf{a} = (a_{10}, ..., a_{i-1,0}, a_{i+1,0}, ..., a_{n0})^T$.

Without loss of generality, we can assume that $\mathbf{a} = 0$. Indeed, if this is not true, then with the help of the change of variables $y_j = x_j + b_j, j \neq i$, we will pass from system (4.2) to a new system in which condition $\mathbf{a} = 0$ is already satisfied.

Now it remains to apply Theorem 2.5 to system (4.2).

Let $\alpha_j(t) = 1 - f_j \sin(x_i(t)) - e_j \cos(x_i(t)); j = 1, ..., n$.

We have that the obtained solutions $x_1(t), ..., x_{i-1}(t), x_{i+1}(t), ..., x_n(t)$ of system (4.2) are bounded. In this case, in the i-th equation

$$\dot{x}_i(t) = \frac{a_{ii}x_i(t)}{1 - f_i \sin(x_i(t)) - e_i \cos(x_i(t))} + \phi(x_1(t), ..., x_n(t))$$

of system (4.2) the function $\phi(x_1(t), ..., x_n(t))$ is also bounded. Finally, by virtue of conditions $a_{ii} < 0$ and $\alpha_i(t) > 0$, we obtain that the solution $x_i(t)$ and all solutions $x_1(t), ..., x_n(t)$ of system (4.2) are bounded. □

Note that Theorem 4.1 admits the following obvious generalization.

Theorem 4.2. *If, under the conditions of Theorem 4.1, the matrix A_i is replaced by a matrix $A = \{a_{ij}\} \in \mathbb{R}^{n\times n}$ such that A is Hurwitz, then the assertion of Theorem 4.1 remains valid.*

In this paper, Theorem 4.2 will not be required. It is presented in order to show how you can expand the modeling capabilities for time series (1.1).

4.1. Algorithm for constructing model (4.2) from known time series

Let us write the equations of system (4.2) in the following form

$$\dot{x}_i(t) = \frac{a_{i1}x_i + \cdots + a_{in}x_n}{1 - f_i \sin(x_i) - e_i \cos(x_i)} = \phi_i(x_1, ..., x_n); i = 1, ..., n. \tag{4.3}$$

Now we rewrite the equations of system (4.3) as follows

$$\begin{aligned} \dot{x}_i(t) &= a_{i1}x_i + \cdots + a_{in}x_n + \dot{x}_i f_i \sin(x_i) + \dot{x}_i e_i \cos(x_i) \\ &= \psi_i(x_1, ..., x_n); i = 1, ..., n. \end{aligned} \tag{4.4}$$

From the point of view of the theory of differential equations, systems (4.3) and (4.4) describe the same dynamics. However, from the point of view of approximation theory (determining the coefficients $a_{i1}, ..., a_{in}, f_i, e_i$ from the known values of the functions $x_i(t), i = 1, ..., n$), these are different problems for systems (4.3) and (4.4).

Indeed, in case of system (4.3) it is necessary to minimize by $a_{11}, ..., e_n$ the loss function $\sum_{i=1}^{n}|\dot{x}_i - \phi_i(x_1, ..., x_n, a_{11}, ..., e_n)|$, and in case of system (4.4) it is necessary to minimize by $a_{11}, ..., e_n$ the loss function $\sum_{i=1}^{n}|\dot{x}_i - \psi_i(x_1, ..., x_n, a_{11}, ..., e_n)|$, where the equations (4.3) are rational and the equations (4.4) are linear.

It is clear that in the case of system (4.4), the approximation problem will be simpler than in the case of system (4.3). That is why we chose system (4.4) for solving the approximation problem. (It should be remembered that the approximation results for system (4.4) may be worse than for system (4.3).)

To simplify the notation, we can assume that in model (4.2) $i = n$.

1. Based on the known time series $\mathbf{x}(t) = \{x_0, x_1, ..., x_N\}$, determine the dimension of the embedding space m and the delay time τ.

2. Based on the known m (here $m = 5$) and τ, construct five time series

$$\mathbf{x}(t) = \{x_0, x_1, x_2, ..., x_L\}, \mathbf{x}(t+\tau) = \{y_0, y_1, y_2, ..., y_L\},$$
$$\mathbf{x}(t+2\tau) = \{z_0, z_1, z_2, ..., z_L\}, \mathbf{x}(t+3\tau) = \{u_0, u_1, u_2, ..., u_L\},$$
$$\mathbf{x}(t+4\tau) = \{v_0, v_1, v_2, ..., v_L\}$$

that are given on the same time interval $T_L \le t_0 + (m-1)\tau \le T$ in equally spaced $L \le N$ nodes: $0, \Delta t, ..., k\Delta t, ..., L\Delta t = T_L \le T$. Thus, $\Delta t = T_L/L$.

3. Fix a learning selections

$$x_0, x_1, ..., x_k; y_0, y_1, ..., y_k; z_0, z_1, ..., z_k; u_0, u_1, ..., u_k; v_0, v_1, ..., v_k,$$

where $36 \le k \le L$.

4. Construct the columns of numerical derivatives D_x, D_y, D_z, D_u, D_v, where

$$D_x = \frac{1}{\Delta t}\begin{pmatrix} x_1 - x_0 \\ \vdots \\ x_k - x_{k-1} \end{pmatrix} \in \mathbb{R}^k, ..., D_v = \frac{1}{\Delta t}\begin{pmatrix} v_1 - v_0 \\ \vdots \\ v_k - v_{k-1} \end{pmatrix} \in \mathbb{R}^k.$$

5. Construct five Jacobi matrices J_x, J_y, J_z, J_u, J_v:

$$J_x = \begin{pmatrix} 1 & x_0 & y_0 & z_0 & u_0 & D_{x1}\sin(v_0) & D_{x1}\cos(v_0) \\ \vdots & \vdots & \vdots & \vdots & \vdots & \vdots & \vdots \\ 1 & x_{k-1} & y_{k-1} & z_{k-1} & u_{k-1} & D_{xk}\sin(v_{k-1}) & D_{xk}\cos(v_{k-1}) \end{pmatrix} \in \mathbb{R}^{k\times 7},$$

....

$$J_u = \begin{pmatrix} 1 & x_0 & y_0 & z_0 & u_0 & D_{u1}\sin(v_0) & D_{u1}\cos(v_0) \\ \vdots & \vdots & \vdots & \vdots & \vdots & \vdots & \vdots \\ 1 & x_{k-1} & y_{k-1} & z_{k-1} & u_{k-1} & D_{uk}\sin(v_{k-1}) & D_{uk}\cos(v_{k-1}) \end{pmatrix} \in \mathbb{R}^{k\times 7},$$

$$J_v = \left(\begin{array}{cccccc|} 1 & x_0 & y_0 & z_0 & u_0 & v_0 \\ \vdots & \vdots & \vdots & \vdots & \vdots & \vdots \\ 1 & x_{k-1} & y_{k-1} & z_{k-1} & u_{k-1} & v_{k-1} \end{array} \right. \rightarrow$$

$$\left| \begin{array}{cc} D_{v1}\sin(v_0) & D_{v1}\cos(v_0) \\ \vdots & \vdots \\ D_{vk}\sin(v_{k-1}) & D_{vk}\cos(v_{k-1}) \end{array} \right) \in \mathbb{R}^{k\times 8}.$$

6. Introduce a vector of unknown parameters

$$\mathbf{p} = (\mathbf{p}_x, ..., \mathbf{p}_v)^T$$

$$= (\underbrace{a_{10}, a_{11}, a_{12}, a_{13}, a_{14}, f_1, e_1}_{\mathbf{p}_x}, ..., \underbrace{a_{50}, a_{51}, a_{52}, a_{53}, a_{54}, a_{55}, f_5, e_5}_{\mathbf{p}_v})^T \in \mathbb{R}^{36}$$

7. Fix the parameters $0 < \varepsilon \leq 1$ and $\lambda > 0$, and minimize the five loss functions (see [29]):

$$\|J_x\mathbf{p}_x - D_x\|_2^2 + \lambda\|\mathbf{p}_x\|_1 \text{ with restriction } \sqrt{f_1^2 + e_1^2} \leq 1 - \varepsilon,$$

$$..., \|J_v\mathbf{p}_v - D_v\|_2^2 + \lambda\|\mathbf{p}_v\|_1 \ \text{ with restriction } \sqrt{f_5^2 + e_5^2} \leq 1 - \varepsilon.$$

8. Using any search optimization method, calculate the vector $\mathbf{p} = \mathbf{p}^* = (\mathbf{p}_x^*, ..., \mathbf{p}_v^*)^T$ whose subvectors $\mathbf{p}_x^*, ..., \mathbf{p}_v^*$ minimize the introduced loss functions.

The results of the operation of this algorithm are presented by the following examples.

$$\begin{cases} \dot{x}(t) = \dfrac{-180.15 - 3.03x + 8.10y + 1.73z + 0.57u}{1 - 0.80\sin(v) - 0.56\cos(v)}, \\ \dot{y}(t) = \dfrac{-58.21 - 10.23x - 3.96y + 13.09z - 2.71u}{1 - 0.70\sin(v) - 0.66\cos(v)}, \\ \dot{z}(t) = \dfrac{22.01 + 0.05x - 12.17y + 1.94z + 9.61u}{1 - 0.90\sin(v) - 0.40\cos(v)}, \\ \dot{u}(t) = \dfrac{219.68 - 2.11x - 0.01y - 10.98z + 4.24u}{1 - 0.71\sin(v) - 0.63\cos(v)}, \\ \dot{v}(t) = \dfrac{199.01 + 3.27x - 4.23y - 1.31z - 7.52u}{1 - 0.40\sin(v) + 0.55\cos(v)}. \end{cases} \tag{4.5}$$

Here initial values are: $x_0 = 91.70, y_0 = -11.01, z_0 = 10.02, u_0 = -10.74, v_0 = 0$.

$$\begin{cases} \dot{x}(t) = \dfrac{138.74 - 7.44x + 15.11y - 0.09z + 2.16u}{1 + 0.80\sin(v) - 0.50\cos(v)}, \\ \dot{y}(t) = \dfrac{80.68 - 12.12x - 1.48y + 13.22z + 0.50u}{1 - 0.70\sin(v) - 0.65\cos(v)}, \\ \dot{z}(t) = \dfrac{-52.62 - 0.52x - 12.38y + 2.88z + 9.01u}{1 - 0.80\sin(v) + 0.40\cos(v)}, \\ \dot{u}(t) = \dfrac{-66.91 - 0.96x - 2.44y - 12.64z + 2.22u}{1 - 0.3\sin(v) + 0.88\cos(v)}, \\ \dot{v}(t) = \dfrac{10 + 2.92x - 3.79y - 1.16z - 10.79u}{1 + 0.30\sin(v) - 0.10\cos(v)}. \end{cases} \tag{4.6}$$

Here initial values are: $x_0 = 11.96, y_0 = -11.01, z_0 = 10.02, u_0 = -10.74, v_0 = 0.$

$$\begin{cases} \dot{x}(t) = \dfrac{145.70 - 7.50x + 15.11y - 0.10z + 2.13u}{1 + 0.80\sin(v) - 0.55\cos(v)}, \\ \dot{y}(t) = \dfrac{81.25 - 12.12x - 2.52y + 13.25z + 0.50u}{1 - 0.71\sin(v) + 0.65\cos(v)}, \\ \dot{z}(t) = \dfrac{-54.11 - 0.53x - 12.38y + 2.88z + 9.02u}{1 - 0.89\sin(v) + 0.42\cos(v)}, \\ \dot{u}(t) = \dfrac{232.55 - 2.34x + 0.34y - 10.71z + 2.97u}{1 - 0.33\sin(v) - 0.88\cos(v)}, \\ \dot{v}(t) = \dfrac{10.12 + 2.91x - 3.79y - 1.16z - 10.77u}{1 - 0.10\sin(v) - 0.30\cos(v)}. \end{cases} \tag{4.7}$$

Here initial values are: $x_0 = 18.70, y_0 = -10.00, z_0 = 85.01, u_0 = -15.00, v_0 = 0.$
(Examples (4.5)-(4.7) of modeling EEG for a sick patient.)

$$\begin{cases} \dot{x}(t) = \dfrac{-1.00 + 0.22x - 7.23y - 5.78z - 8.15u}{1 - 0.78\sin(v) - 0.56\cos(v)}, \\ \dot{y}(t) = \dfrac{-0.00 + 4.19x - 0.57y - 2.96z - 5.75u}{1 - 0.77\sin(v) + 0.56\cos(v)}, \\ \dot{z}(t) = \dfrac{1.22 + 2.73x + 3.26y - 0.14z - 2.44u}{1 - 0.29\sin(v) + 0.14\cos(v)}, \\ \dot{u}(t) = \dfrac{0.34 + 7.00x + 6.91y + 5.10z - 0.30u}{1 - 0.67\sin(v) - 0.43\cos(v)}, \\ \dot{v}(t) = \dfrac{17.32 - 4.82x + 0.56y + 0.87z + 3.58u}{1 + 0.87\sin(v) + 0.20\cos(v)}. \end{cases} \tag{4.8}$$

Here initial values are: $x_0 = 1.70, y_0 = 6.06, z_0 = 11.41, u_0 = -10.21, v_0 = 0.$

$$\begin{cases} \dot{x}(t) = \dfrac{9.61 - 0.74x + 2.74y + 2.51z - 3.73u}{1 + 0.78\sin(v) + 0.46\cos(v)}, \\ \dot{y}(t) = \dfrac{17.22 - 3.04x - 0.187y + 2.61z + 2.05u}{1 - 0.64\sin(v) + 0.36\cos(v)}, \\ \dot{z}(t) = \dfrac{-0.04 - 2.52x - 2.05y + 0.36z + 3.49u}{1 - 0.79\sin(v) + 0.14\cos(v)}, \\ \dot{u}(t) = \dfrac{-9.04 + 3.43x - 2.06y - 2.90z - 0.04u}{1 - 0.82\sin(v) - 0.43\cos(v)}, \\ \dot{v}(t) = \dfrac{-2.18 - 4.05x + 4.08y - 1.91z - 2.27u}{1 + 0.30\sin(v) - 0.40\cos(v)}. \end{cases} \tag{4.9}$$

Here initial values are: $x_0 = -21.70, y_0 = -1.26, z_0 = 10.07, u_0 = -10.21, v_0 = 0.$

$$\begin{cases} \dot{x}(t) = \dfrac{24.51 - 0.92x + 2.45y + 2.93z - 4.37u}{1 - 0.48\sin(v) - 0.56\cos(v)}, \\ \dot{y}(t) = \dfrac{31.81 - 2.80x - 1.35y + 2.50z + 2.06u}{1 - 0.47\sin(v) + 0.56\cos(v)}, \\ \dot{z}(t) = \dfrac{7.74 - 3.70x - 0.53y + 0.58z + 3.50u}{1 - 0.90\sin(v) + 0.40\cos(v)}, \\ \dot{u}(t) = \dfrac{-3.40 + 3.44x - 1.02y - 2.70z - 3.86u}{1 - 0.71\sin(v) - 0.63\cos(v)}, \\ \dot{v}(t) = \dfrac{-23.18 - 4.12x + 3.22y - 1.70z - 1.99u}{1 - 0.0\sin(v) - 0.0\cos(v)}. \end{cases} \tag{4.10}$$

Here initial values are: $x_0 = 40.02, y_0 = 33.43, z_0 = -11.21, u_0 = 7.62, v_0 = 0.$ (Examples (4.8)-(4.10) of modeling the EEG for a healthy patient.)

It should be said that in all the above examples, the solution $v(t)$ is unbounded (it oscillates around the straight line $v = a_{50}t$). In this case, we get a contradiction with the time series $v_0, v_1, v_2, ...$, which is built from the bounded series $x_0, x_1, x_2, ...$, and therefore must also be bounded.

This contradiction can be removed in the following way. For example, let's replace the fifth equation of system (4.9) with the equation

$$\dot{v}(t) = \frac{-2.18 - 4.05x + 4.08y - 1.91z - 2.27u + a_{55}v}{1 + 0.30\sin(v) - 0.40\cos(v)}. \tag{4.11}$$

Consider the graphs of the trajectory $v(t)$ at $a_{55} = 0$ and $a_{55} \neq 0$:

Comparing graphs Fig.4.2(b2) and Fig.4.3(a4) , it can be seen that the behavior of the curves presented in these graphs is similar. We add that the behavior of the curves $x(t), y(t), z(t)$ and $u(t)$ obtained from the system (4.9) and the behavior of the same curves obtained from the system (4.9), taking into account (4.11), is also similar. As for quantitative differences, we note that the variable $v(t)$ is included in the first four equations of system (4.9) (and the same system, but with equation (4.11)) only in complex $\alpha_i(t) = 1 - f_i\sin(v(t)) - e_i\cos(v(t))$, where $0 < \alpha_i(t) < 2; i = 1, ..., 5$. The last restriction gives quantitative differences in the solutions of system (4.9) (and the same system, but with equation (4.11)).

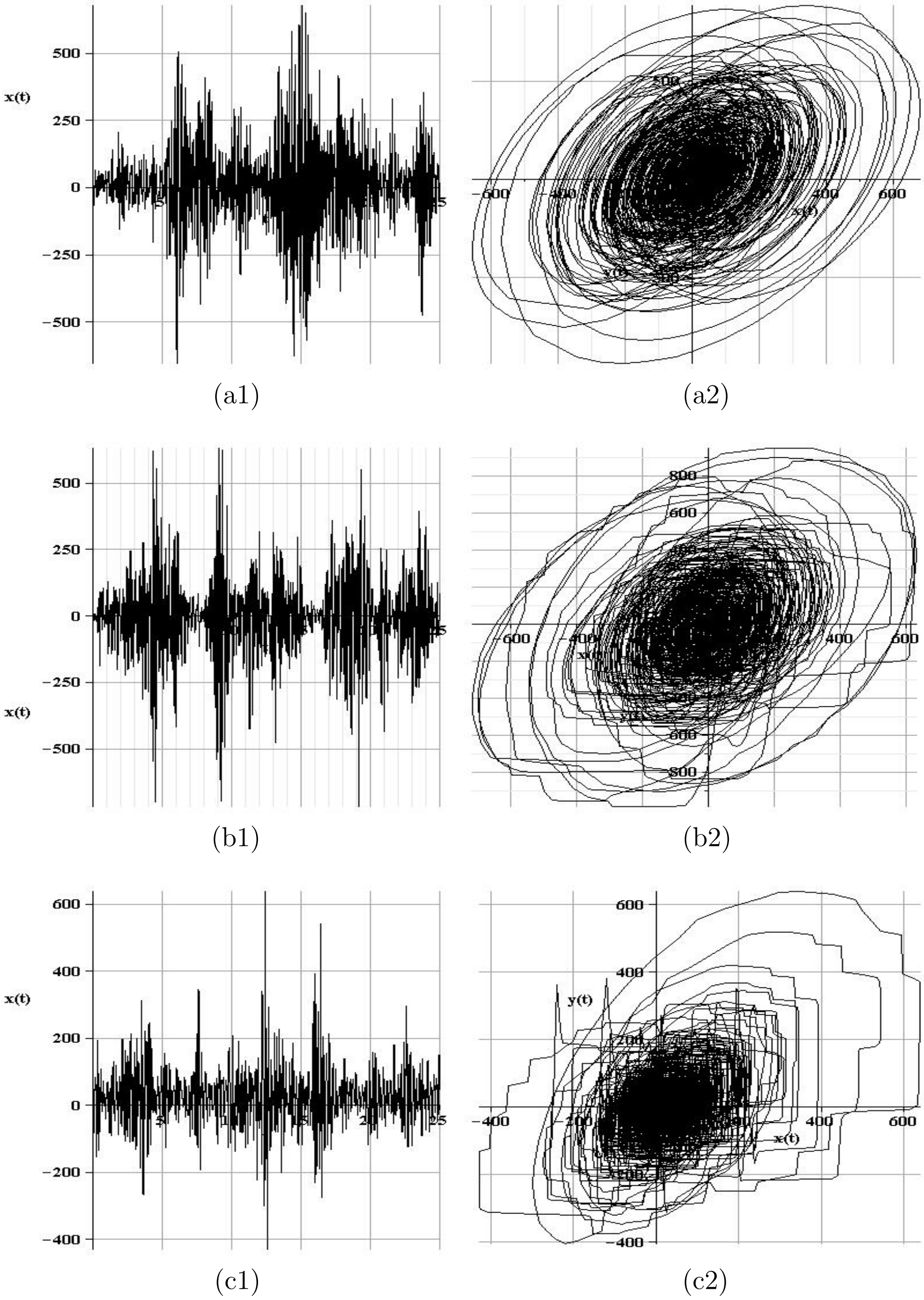

Fig. 4.1. The electroencephalogram taken from a specific point in the cerebral cortex of the patient with an epileptic disease: at points 1-500 of time series (1.1), (a1) in coordinates $(x(t), t)$ and (a2) in coordinates $(x(t), x(t+\tau))$; at points 501-1000 of time series (1.1), (b1) in coordinates $(x(t), t)$ and (b2) in coordinates $(x(t), x(t+\tau))$; at points 2001-2500 of time series (1.1), (c1) in coordinates $(x(t), t)$ and (c2) in coordinates $(x(t), x(t+\tau))$.

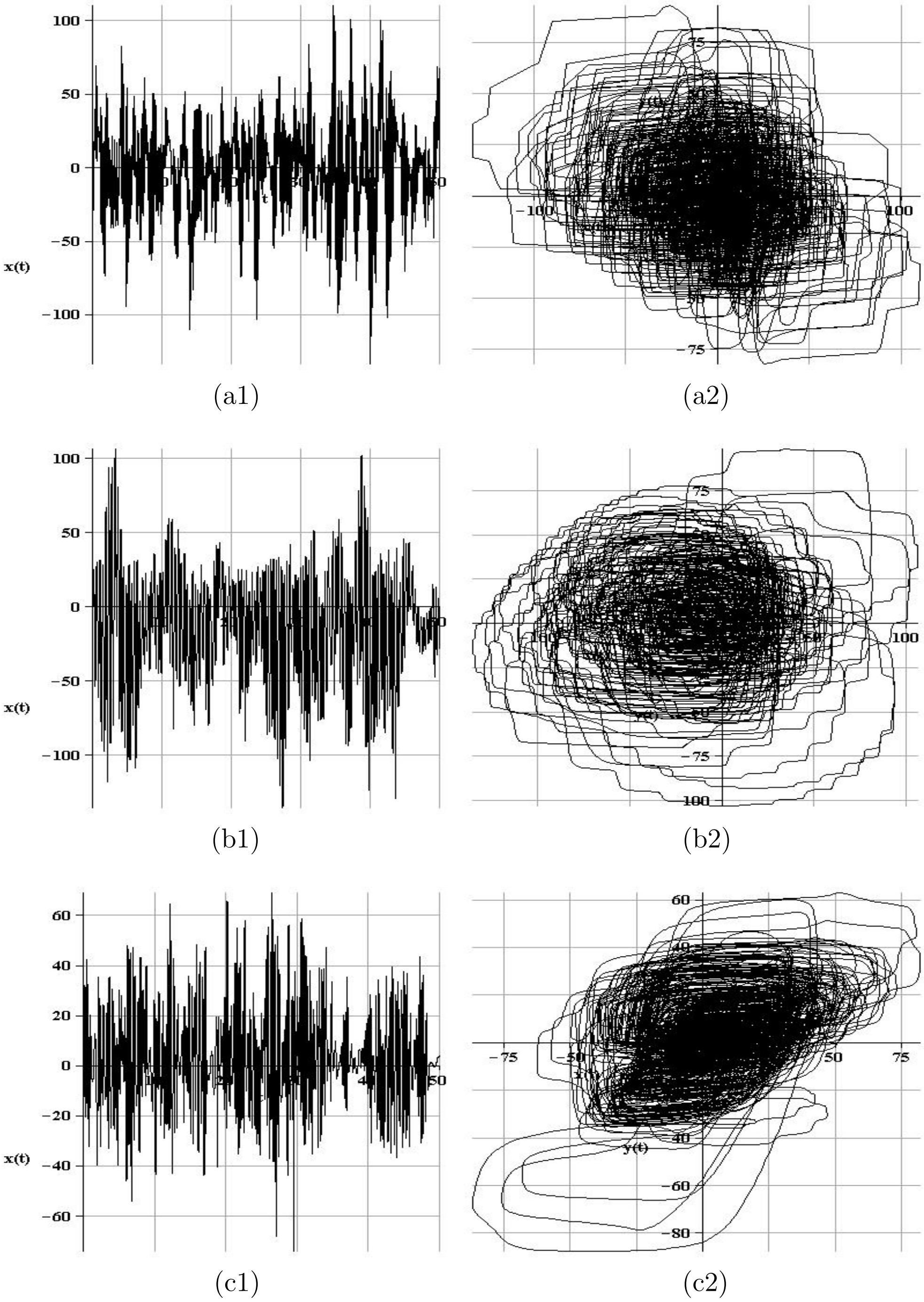

Fig. 4.2. The electroencephalogram taken from a specific point in the cerebral cortex of a healthy patient: at points 1-500 of time series (1.1), (a1) in coordinates $(x(t), t)$ and (a2) in coordinates $(x(t), x(t+\tau))$; at points 501-1000 of time series (1.1), (b1) in coordinates $(x(t), t)$ and (b2) in coordinates $(x(t), x(t+\tau))$; at points 1-4065 of time series (1.1), (c1) in coordinates $(x(t), t)$ and (c2) in coordinates $(x(t), x(t+\tau))$.

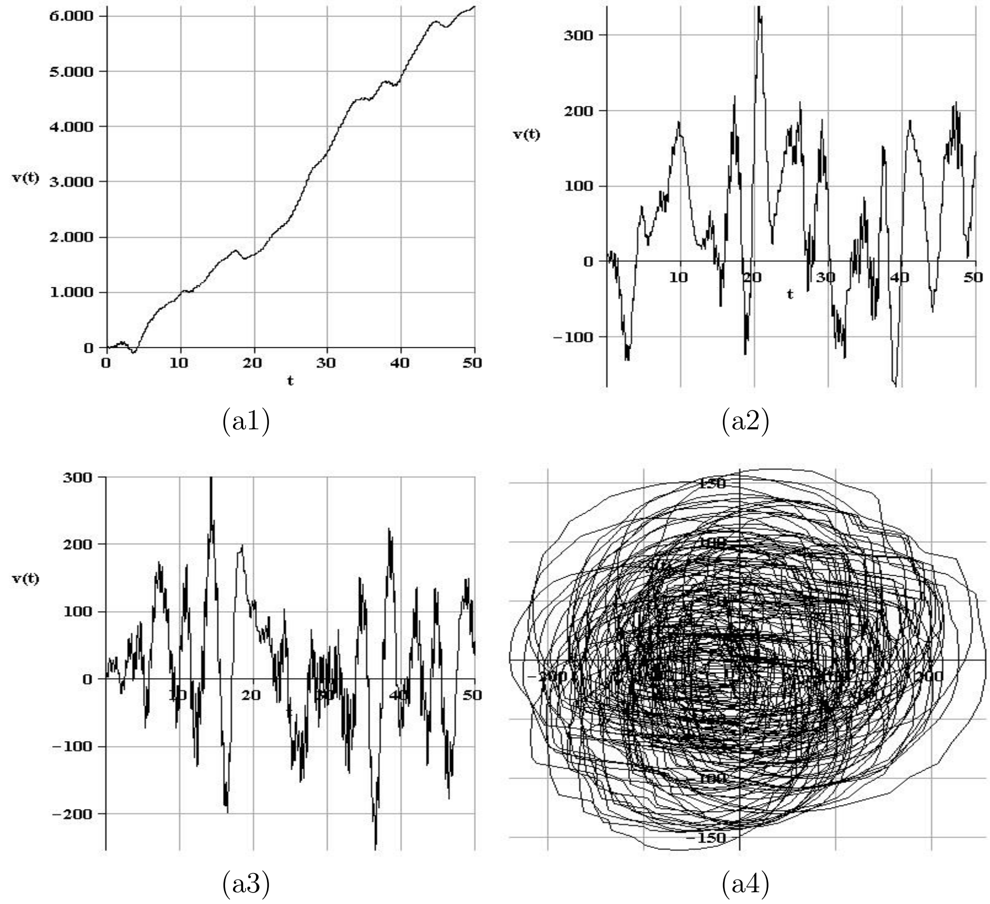

Fig. 4.3. Graphs of the variable $v(t)$ from equation (4.11): (a1) $a_{55} = 0$; (a2) $a_{55} = -1$; (a3) $a_{55} = -2$. Graph of the projection of the phase trajectory of system (4.9) with equation (4.11) onto plane (x, y) at $a_{55} = -2$ (a4).

To complete the simulation, it is necessary to analyze the Lyapunov exponents for the time series presented in Fig.2.1(a1,a2) [21].

Before starting the calculations of Lyapunov exponents, sectioning of each of the time series shown in Fig.2.1(a1) and Fig.2.1(a2) was carried out.

Each time series consists of 4065 points. This set of points was divided into 4 disjoint subsets (≈ 1000 points each). Thus, we get the following differences.

1. The Lyapunov exponents for a sick patient have greater modulo values than the same exponents for a healthy patient. (The number of positive Lyapunov exponents for a sick patient is 2. For a healthy patient, the same number varies from 2 to 3. Thus, both processes shown in Fig.2.1 are hyperchaotic.)

2. The dimension of the embedding space of a sick patient for each section is $m = 4$ or $m = 5$. At the same time, the dimension of the embedding space of a healthy patient for similar sections varies from $m = 4$ to $m = 6$.

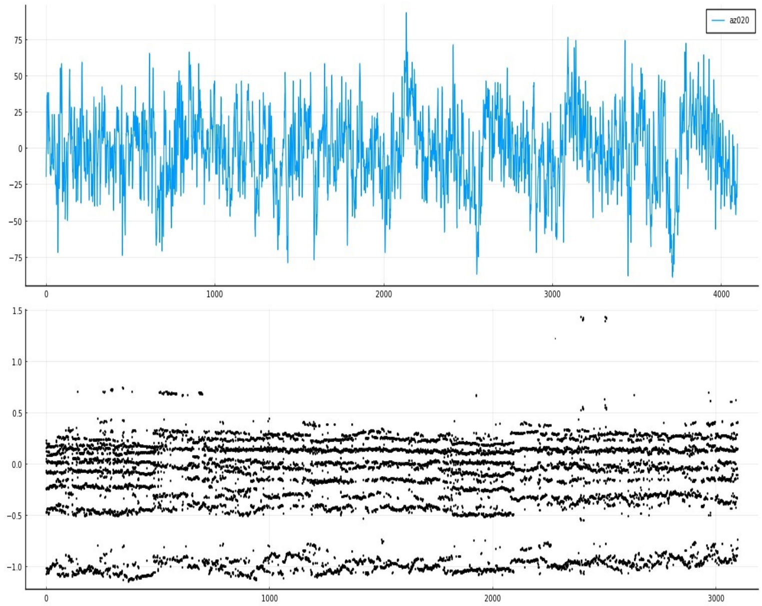

Fig. 4.4. The electroencephalogram Fig.2.1(a1) and the distribution of its Lyapunov exponents for time series (1.1)

3. Now let's compare the experimental Lyapunov exponents (Fig.4.4, Fig.4.5) and the Lyapunov exponents of dynamic systems (4.6) and (4.9) simulating the corresponding time series (see Fig.4.6).

Let $\Lambda_1 \geq ... \geq \Lambda_n$ are the Lyapunov exponents for a dynamical system in $\mathbb{R}^n$. Assume that j is the largest integer for which $\Lambda_1 + \cdots + \Lambda_j \geq 0$. The Kaplan-Yorke dimension is given by the formula [30, 31]:

$$d_{KL} = j + \frac{\Lambda_1 + \cdots + \Lambda_j}{|\Lambda_{j+1}|}. \tag{4.12}$$

In the equations (4.5)-(4.10), for coordinate $v(t)$, we have $v(t) \to \infty$ or $v(t) \to -\infty$ as $t \to \infty$ (see Fig.4.3). This means that systems (4.5)-(4.10) behave as nonstationary. Therefore, it is necessary to consider the attractors of these systems as projections along the axis v onto a 4-dimensional subspace $(x, y, z, u) \in \mathbb{R}^5$. In this case, the dimension of the attractor in this case will be less than 4.

Let's compare the fractal dimensions of the attractors presented in Fig.2.2 and Fig.4.1, Fig.4.2 calculated by formula (4.12).

Taking into account Fig.4.4, we have two situations: 1) $\Lambda_1 \approx 0.3, \Lambda_2 \approx 0.25$, $\Lambda_3 \approx 0.2, \Lambda_4 \approx 0.0, \Lambda_5 \approx -1.0$; from here it follows that $d_{KL} \approx 4.75$. 2) $\Lambda_1 \approx 0.25, \Lambda_2 \approx 0.15, \Lambda_3 \approx 0.0, \Lambda_4 \approx -0.25, \Lambda_5 \approx -0.5, \Lambda_6 \approx -1.0$; here we have $d_{KL} \approx 4.6$.

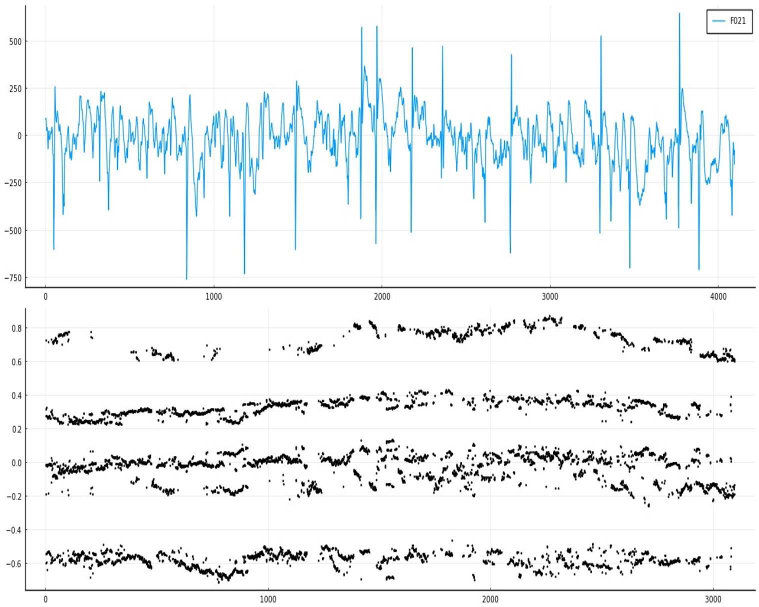

Fig. 4.5. The electroencephalogram Fig.2.1(a2) and the distribution of its Lyapunov exponents for time series (1.1)

Taking into account Fig.4.5, we have: 1) $\Lambda_1 \approx 0.6, \Lambda_2 \approx 0.03, \Lambda_3 \approx 0.0, \Lambda_4 \approx -0.7$; from here it follows that $d_{KL} \approx 3.9$ or 2) $\Lambda_1 \approx 0.6, \Lambda_2 \approx 0.2, \Lambda_3 \approx 0.0, \Lambda_4 \approx -0.2, \Lambda_5 \approx -0.7$; from here it follows that $d_{KL} \approx 7.0$.

Thus, the fractal dimension of the healthy patient attractor is greater than that of the sick one. This statement also holds for the attractors of model system (4.6) (for Fig.4.6(a1), we have $\Lambda_1 \approx 0.11$, $\Lambda_2 \approx -0.07, \Lambda_3 \approx -0.31, \Lambda_4 \approx -0.82$; here $d_{KL} \approx 2.8$) and model system (4.9) (for Fig.4.6 (a2), we have $\Lambda_1 \approx 0.19, \Lambda_2 \approx 0.03$, $\Lambda_3 = -0.13, \Lambda_4 = -0.51$; here $d_{KL} \approx 3.7$). The only question is: why is the dimension of the sick patient attractor greater than $m = 5$? The fact is that when calculating the Lyapunov exponents for time series, the noise component plays an important role. Its presence gives an overestimated value of the fractal dimension (especially for the attractor of a sick patient).

This suggests that the chaos generated by the signals of the cerebral cortex of a healthy patient has a more complex structure than the chaos generated by the signals of the cerebral cortex of a sick patient. The same statement can be confirmed by comparing Fig.4.1(a2),(b2),(c2) and Fig.4.2(a2),(b2),(c2).

In addition, we note that attractors are not explicitly represented in these figures, but can be constructed from trajectories (see [2]). In both cases, the normal activity is the internal trajectory (solid black area; see Fig.4.1 and Fig.4.2), and the seizure is the external trajectory (higher amplitude activity; sparse area formed by a single trajectory; see Fig.4.1).

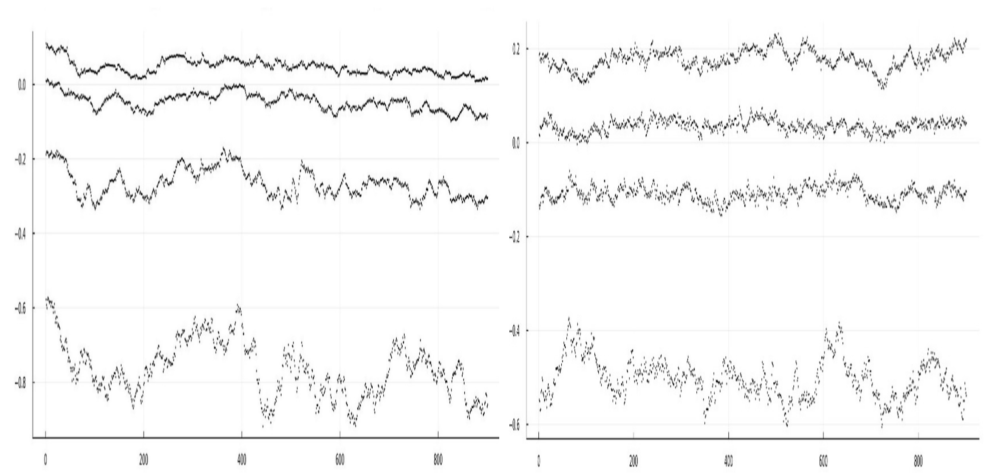

(a1) (a2)

Fig. 4.6. Distribution of Lyapunov exponents for model (4.6) (a1) and model (4.9) (a2). Here $m = 4$ is less than the dimension $m = 5$ of the real embedding space (see Fig.4.5). This means that different models (see Fig.4.3) must be used for different measurement intervals.

5. On the existence of limit cycles in system (4.2)

It is known that chaotic processes in dynamical systems usually begin with a cascade of bifurcations of limit cycles (Feigenbaum's scenario of doubling the period [32]). Since the processes presented on any EEG are clearly chaotic (see the figures of this article), it is necessary to show that model (4.2) , at certain values of the coefficients, generates a limit cycle.

Consider the following simplest version of system (4.2) for $n = 2$:

$$\dot{x}_1(t) = \frac{a_{11}x_1 + a_{12}x_2}{1 - \varepsilon_1 \cos(x_1)}, \dot{x}_2(t) = \frac{a_{21}x_1 + a_{22}x_2}{1 - \varepsilon_2 \cos(x_2)}. \tag{5.1}$$

We introduce a matrix $S = \{s_{ij}\} \in \mathbb{R}^{2\times 2}$ such that either

$$S^{-1}AS = \begin{pmatrix} \lambda_1 & 0 \\ 0 & \lambda_2 \end{pmatrix} \text{ or } S^{-1}AS = \begin{pmatrix} \lambda & \mu \\ -\mu & \lambda \end{pmatrix}, \tag{5.2}$$

where $A = \{a_{ij}\} \in \mathbb{R}^{2\times 2}$ and $\det A \neq 0$.

Now we introduce a change of variables $x_1 = s_{11}y_1 + s_{12}y_2, x_2 = s_{21}y_1 + s_{22}y_2$ in system (5.1) and construct the following function

$$V = \frac{y_1^2 + y_2^2}{2}.$$

Then, taking into account (5.2), we get

$$\dot{V}_t = \lambda_1 y_1^2 + \lambda_2 y_2^2 + \frac{\phi_1(y_1, y_2)\cos(s_{11}y_1 + s_{12}y_2) + \phi_2(y_1, y_2)\cos(s_{21}y_1 + s_{22}y_2)}{|\varepsilon_1|^{-1} - \cos(s_{11}y_1 + s_{12}y_2)}$$

$$+\frac{\psi_1(y_1,y_2)\cos(s_{11}y_1+s_{12}y_2)+\psi_2(y_1,y_2)\cos(s_{21}y_1+s_{22}y_2)}{|\varepsilon_2|^{-1}-\cos(s_{21}y_1+s_{22}y_2)}.$$

(Here $\phi_i(y_1,y_2), \psi_i(y_1,y_2)$ are quadratic forms, $|\varepsilon_i| < 1$; $i = 1,2$. The situation $\lambda_1 = \lambda_2 = \lambda$ is not excluded.)

Let us introduce the set $\mathbb{H} = \{(y_1,y_2)^T \in \mathbb{R}^2 | \dot{V}_t \geq 0\}$ and the boundary $\mathbb{L} = \{(y_1,y_2)^T \in \mathbb{R}^2 | \dot{V}_t = 0\}$ of this set. Now we use Theorem 2.5. Since the matrix A is Hurwitz, then $\lambda_1 < 0, \lambda_2 < 0$. Consider the behavior of the function $V(y_1,y_2)$ on the line $s_{11}y_1 + s_{12}y_2 = s_{21}y_1 + s_{22}y_2 = (2k+1)\pi/2$, where $k = 0 \pm 1, \pm 2, \ldots$. Obviously, if $k \to \infty$, then $s_{11}y_1 + s_{12}y_2 = s_{21}y_1 + s_{22}y_2 = (2k+1)\pi/2 \to \infty$. In this case $\dot{V}_t(y_1,y_2) \to \lambda_1 y_1^2 + \lambda_2 y_2^2 < 0$ and the nonnegative function $V(y_1,y_2)$ is decreasing along the mentioned straight line.

It is clear that there must be a moment $t_c > 0$ such that $\dot{V}_t(y_1(t_c), y_2(t_c)) = 0$. From here it follows that the boundary $\mathbb{L}$ of the set $\mathbb{H}$ is closed and the set itself is a compact positively invariant set with respect to (5.1). Thus, all the conditions of Theorem 2.2 [25] are satisfied and the set $\mathbb{L}$ contains a stable limit cycle (see Fig.5.1). (If $(y_1,y_2)^T \in \mathbb{H}$, then $\dot{V}_t(y_1,y_2) \geq 0$ and the unique equilibrium point $(0,0)^T \in \mathbb{H}$ is a repeller. Therefore, the trajectory $(y_1(t), y_2(t))^T$ is attracted to some set $\mathbb{C} \subset \mathbb{L}$, which must be the limit cycle.)

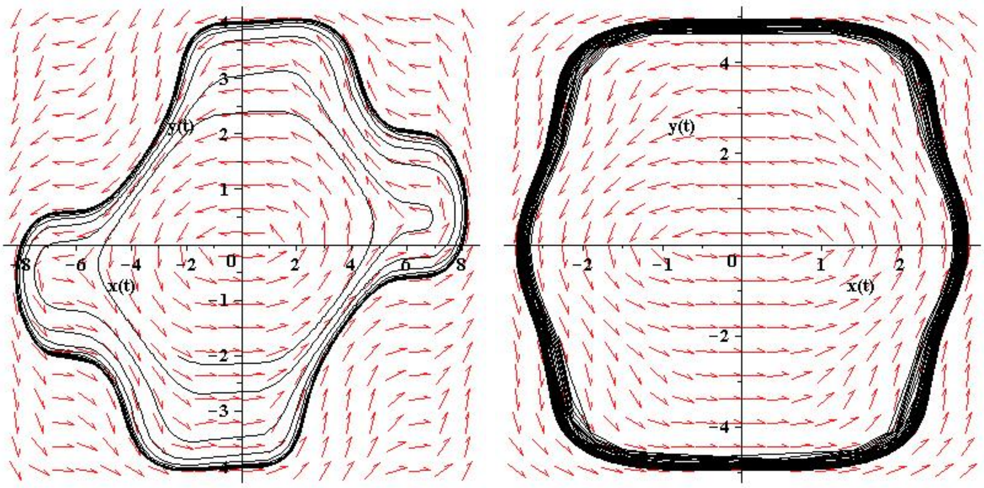

(a1) (a2)

Fig. 5.1. Limit cycles of system (5.1) at the following parameter values: (a1) $a_{11} = 0.52, a_{12} = -7.23, a_{21} = 1.19, a_{22} = -0.57, \varepsilon_1 = 0.99, \varepsilon_2 = -0.85$; (a2) $a_{11} = 0.36, a_{12} = -10.21, a_{21} = 15.22, a_{22} = -0.37, \varepsilon_1 = 0.97, \varepsilon_2 = -0.87$. Here $x(t) = x_1(t), y(t) = x_2(t)$.

6. Conclusion

The paper presents new models (2.2), (2.3), (2.4), (4.1), and (4.2) describing strongly oscillating processes. As an application of one of these models (this is system (4.2)), the problem of modeling signals arising in the cerebral cortex, in particular, signals arising in epilepsy, was considered. It is shown that the constructed model distinguishes quite well the signals generated by the brain of a healthy patient and a patient with epilepsy.

However, the question of using model (4.2) for the diagnosis of epilepsy remains open. The fact is that the model (4.2) does not give accurate quantitative characteristics of epileptic seizures occurring in the cerebral cortex of a sick patient. In our opinion, this is due to the fact that rather crude computational tools are used to tune the model parameters (4.2): least squares method, methods LASSO, SIND [14, 29], and so on. Therefore, to improve the quality of modeling, it is necessary to use a more powerful tool. This tool is recurrent neural networks.

The use of neural networks will bring the quality of modeling to such a state in which it will be possible to take bifurcation analysis [9, 16] to study system (4.2). In this case, we will be able to connect the values of the coefficients of model (4.2) with the parameters of EEG, and hence with the real state of the sick patient.

At the moment, model (4.2) makes it possible to distinguish between healthy and sick patients only (without detailing their states): in a sick patient, the amplitude of signal oscillations is several times greater than in a healthy patient.

Why model (4.2) is presented in this form? There are three main reasons:

1. The electroencephalogram $x(t)$ shows that the electrical processes occurring in the cerebral cortex have a strongly oscillating, almost periodic nature. This means that there is a sequence of times $t_1, t_2, ...$ such that the modules of the derivatives $|\dot{x}(t_1)|, |\dot{x}(t_2)|, ...$ increase sharply. It is this fact that is taken into account in the proposed form of denominators in systems (2.2) and (4.2).

2. The calculated variables $x_2(t), x_3(t), ...$ are obtained from the experimental dependence $x_i(t) = x(t)$ using the delay method [6, 9] (here $i = 1$). This means that the jump moments of the derivatives $\dot{x}(t_1), \dot{x}(t_2)$, of the function $x_1(t)$ must be shifted for the functions $x_2(t) = x_1(t+\tau), x_3(t) = x_1(t+2\tau), ...$ by τ: $t_1 + \tau, t_1 + 2\tau, ..., t_2 + \tau, t_2 + 2\tau, ...$ That is why the terms in the denominators of the equations of system (4.2) are linear combinations of the terms of only one denominator $1 - f_1 \sin(x_1(t)) - e_1 \cos(x_1(t))$. (In system (4.2), any function $x_i(t)$ can be taken as an experimental variable; $i \in \{1, ..., n\}$. In examples (4.5)–(4.10) $i = 5$.)

3. In all denominators of equations (2.4) in the role of the function $\cos(t)$ any periodic function can be taken. Let us assume that the amplitude of oscillations of this function is A. Then in all equations (2.4) parameter ε_i must be replaced by parameter $\varepsilon_i/A; i = 1, ..., n$.

In conclusion, let us say a few words about future studies of epilepsy models.

First of all, we note one important circumstance. All real EEGs are usually very noisy. Therefore, before modeling, it will be necessary to filter the data obtained from these EEGs.

The standard filtering process is to cut large amplitudes (jumps). However, in our situation, such a process must be carried out very carefully: filtering can remove amplitudes that are critical for diagnosis. (In this case, the introduction of functions (2.1) would be unjustified.)

As previous studies have shown, it is impossible to build one model that would approximate the entire time series. Therefore, along with filtering, the question of sectioning the time series also arises. This sectioning should be done in such a way that only one model is used to model each section of the series.

Let i be any number from the set $\{1, ..., n\}$. In the present work, model

$$\begin{cases} \dot{x}_1(t) = \dfrac{a_{10} + a_{11}x_1 + \cdots + a_{1n}x_n}{1 + \varepsilon_1 \cdot \cos(x_i + \alpha_1)}, \\ \quad . \ . \ . \ . \ . \ . \ . \ . \ . \ . \ . \ . \ . \ . \ . \ . \ . \ , \\ \dot{x}_i(t) = \dfrac{a_{i0} + a_{i1}x_1 + \cdots + a_{in}x_n}{1 + \varepsilon_i \cdot \cos(x_i + \alpha_i)}, \\ \quad . \ . \ . \ . \ . \ . \ . \ . \ . \ . \ . \ . \ . \ . \ . \ . \ . \ , \\ \dot{x}_n(t) = \dfrac{a_{n0} + a_{n1}x_1 + \cdots + a_{nn}x_n}{1 + \varepsilon_n \cdot \cos(x_i + \alpha_n)} \end{cases} \tag{6.1}$$

was investigated. (There are $n^2 + 3n$ parameters $a_{10}, a_{1n} ..., a_{nn}, \varepsilon_1, \alpha_1, ..., \varepsilon_n, \alpha_n$.)

The next step is to explore the universal model

$$\begin{cases} \dot{x}_1(t) = \dfrac{a_{10} + a_{11}x_1 + \cdots + a_{1n}x_n}{1 + \varepsilon_1 \cdot \cos(b_{11}x_1 + \cdots + b_{1n}x_n + \gamma_1)}, \\ \quad . \ , \\ \dot{x}_n(t) = \dfrac{a_{n0} + a_{n1}x_1 + \cdots + a_{nn}x_n}{1 + \varepsilon_n \cdot \cos(b_{n1}x_n + \cdots + b_{nn}x_n + \gamma_n)} \end{cases} \tag{6.2}$$

(There are $2n^2 + 3n$ parameters $a_{10}, a_{1n} ..., a_{nn}, b_{11}, ..., b_{nn}, \varepsilon_1, \gamma_1, ..., \varepsilon_n, \gamma_n$.)

Finally, we note that it is possible to propose a model that generalizes models (6.1) and (6.2):

$$\begin{cases} \dot{x}_1(t) = \dfrac{a_{10} + a_{11}x_1 + \cdots + a_{1n}x_n}{1 + \varepsilon_1 \cdot \cos(h_1(x_1, ..., x_n))}, \\ \quad . \ . \ . \ . \ . \ . \ . \ . \ . \ . \ . \ . \ . \ . \ . \ . \ . \ . \ , \\ \dot{x}_n(t) = \dfrac{a_{n0} + a_{n1}x_1 + \cdots + a_{nn}x_n}{1 + \varepsilon_n \cdot \cos(h_n(x_n, ..., x_n))}, \end{cases} \tag{6.3}$$

where $h_i(x_n, ..., x_n); i = 1, ..., n$, are continuous functions of their arguments.

In order to guarantee the boundedness of solutions of systems (6.1), (6.2), and (6.3) the following conditions:

1. The matrix $A = \{a_{ij}\}; i, j = 1, ..., n$, is Hurwitz;

2. The parameters $|\varepsilon_i| < 1; i = 1, ..., n$,

must be satisfied. (The proof of the last assertion almost completely repeats the proof of Theorem 2.5. Therefore, there is no need to give it again.)

The fulfillment of these conditions makes it possible to vary the parameters of systems (6.1), (6.2), and (6.3) within a very wide range, which guarantees the absence of unbounded solutions (a mandatory condition for any simulation).

We hope that the use of recurrent neural networks to adjust the coefficients of systems (6.1) and (6.2) will lead to more adequate models of epilepsy than the models discussed in this article.

References

1. V. Ye. Belozyorov, O. V. Pohorielov, V. N. Serdiuk, V. G. Zaytsev, *New approach to problem of diagnostics of cerebral cortex diseases using chaotic dynamics methods*, *In: The collection of 7 th The international conference "Social Science and Humanity"*, September 23–29, London, **2**(2017), 7–28.
2. W. W. Lytton, *Computer modeling of epilepsy*, *Nature Reviews Neuroscience*, **9**(8)(2008), 626–637.
3. D. A. Torse, R. Khanai, V. V. Desai, *Classification of epileptic seizures using recurrence plots and machine learning techniques*, *Proceedings of the 2019 IEEE International Conference on Communication and Signal Processing (ICCSP)*, April (2019), India, 1-6, https://ieeexplore.ieee.org/document/8697965.
4. D. A. Torse, R. Khanai, K. Pai, S. Iyer, *Hardware implementation of automated seizure detection system using EEG signals and edge computing*, *Proceedings of the IEEE Sixth International Conference on Trends in Electronics and Informatics (ICOEI 2022)*, April (2022), India, https://ieeexplore.ieee.org/xpl/conhome /9776594/proceeding, 470–475.
5. V. Raju, V. Malsoru, K. Srinivas, B. K. Rani, G. Madhukar, *Nonlinear dynamical systems to study epileptic seizures and extract average amount of mutual information from encephalographs* , *IP Indian Journal of Neurosciences*, **8**(4)(2022), 254–259.
6. C. L. Webber, N. Marwan (eds), *Reccurence Quantification Analysis. Theory and Best Practice*, Springer, NY, Dordrecht, Heidelberg, London, 2015.
7. R. V. Donner, Y. Yong Zou, Y. F. Donges, N. Marwan, J. Kurths, *Recurrence networks - a novel paradigm for nonlinear time series analysis*, *New Journal of Physics*, **12**(2010), Article ID 033025, 40 pages.
8. J. -P. Eckmann, S. Kamphorst, D. Ruelle, *Recurrence plots of dynamical systems*, *Europhysics Letters*, **4**(1987), 973–977.
9. H. Kantz, T. Schreiber, *Nonlinear Time Series Analysis - 2nd Edition*, Cambridge University Press, Cambridge, 2004.
10. N. Marwan, M.Romano, M. Thiel, J. Kurths, *Recurrence plots for the analysis of complex systems*, *Physics Reports*, **438**(2007), 237–329.
11. N. Marwan, *How to avoid pitfalls in recurrence plot based data analysis*, *International Journal of Bifurcation and Chaos*, **21**(2011), 1003–1017.
12. A. P. Shultz, Y. Zou, N. Marwan, M. T. Turvey, *Local minima-based recurrence plots for continuous dynamical systems*, *International Journal of Bifurcation and Chaos*, **21**(2011), 1065–1075.
13. J. P. Zbilut, C. I. Webber, *Embeddings and delays as derived from quantification of recurrence plots*, *Physics Letters A*, **171**(1992), 199–203.
14. N. M. Mangan, S. L. Brunton, J. L. Proctor, J. N. Kutz, *Inferring biological networks by sparse identification of nonlinear dynamics*, *IEEE Transactions on Molecular, Biological, and Multi-Scale Communications*, **2**(1)(2016), 52–63.

15. C. K. Ye, *Recurrence analysis of time series*, *A project report submitted in partial fulfilment of the requirements for the award of Bachelor of Science (Hons.) Applied Mathematics With Computing*, Faculty of Engineering and Science Universiti Tunku Abdul Rahman, April (2019), Malaysia, http://eprints.utar.edu.my/3383/, 1–59.
16. Y. -C. Lai, N. Ye, *Recent developments in chaotic time series analysis*, *Int. J. Bifurcation and Chaos*,**13**(2003), 1383–1422.
17. M. Li, *Fractal time series – a tutorial review*, *Mathematical Problems in Engineering*, **2010**(2019), Article ID 157264, 26 pages.
18. Z. Liu, *Chaotic time serias analysis*, *Mathematical Problems in Engineering*, **2010**(2010), Article ID 720190, 31 pages.
19. F. K. Fuss, *A robust algorithm for optimization and customization of fractal dimensions of time series modified by nonlinearly scaling their time derivatives: mathematical theory and practical applications*, Computational and Mathematical Methods in Medicine, **2013**(2913), Article ID 178476, 19 pages.
20. Y. H. Li, X. J. Tian, X. Q. Li, *Nonlinear second-order model and equilibrium point characteristic analysis of DC traction power supply system*, *ISRN* Applied Mathematics, **2013**(2013), Article ID 981692, 8 pages.
21. V. Ye. Belozyorov, D. V. Dantsev, Y. V. Koshel, *On the equivalence of real dynamic process and its models*, *Journal of Optimization, Differential Equations and Their Applications (JODEA)*, **29**(2)(2021), 76–91.
22. V. Ye. Belozyorov, D. V. Dantsev, *Modeling of chaotic processes by means of antisymmetric neural ODEs*, *Journal of Optimization, Differential Equations and Their Applications (JODEA)*, **30**(1)(2022), 1–41.
23. V. Ye. Belozyorov, Ye. M. Kosariev, M. M. Pulin, V. G. Sychenko, V. G. Zaytsev. *A new mathematical model of dynamic process in direct current traction power supply system*, *Journal of Optimization, Differential Equations and Their Applications (JODEA)*, **27**(1) (2019), 21–55.
24. Toolboxes for Complex Systems, *Potsdam Institute for Climate Impact Research (PIK)*, Germany, http://tocsy.pik-potsdam.de.
25. V. Ye. Belozyorov, D. V. Dantsev, *Stability of neural ordinary differential equations with power nonlinearities*, *Journal of Optimization, Differential Equations and Their Applications (JODEA)*, **28**(2)(2020), 21–46.
26. B. P. Demidovich, *Lectures on the mathematical stability theory*, Nauka, Moscow, 1967 (in Russian).
27. H. K. Khalil, *Nonlinear Systems – 2nd Edition*, Prentice Hall, New-Jersy, 1996.
28. F. Takens, *Detecting strange attractors in turbulence*, *Lecture Notes in Mathematics* , Springer-Verlag, NY, Berlin, **898**(1981), 366–381.
29. Q. Qu, J. Sun, *Finding a sparse vector in a subspace: linear sparsity using alternating directions*, *arXiv preprint arXiv:1412.4659v3[cs.IT]*, (2016), 1–39.
30. S. P. Banks, *Analysis and structure of a new chaotic system*, International Journal of Bifurcation and Chaos, **9**(8) (1999), 1571–1583.
31. V. Ye. Belozyorov, S. A. Volkova, *Odd and even functions in the design problem of new chaotic attractors*, International Journal of Bifurcation and Chaos, **32**, (2022), Article ID 2250218, 26 pages.
32. V. Ye. Belozyorov, *Universal approach to the problem of emergence of chaos in autonomous dynamical systems*, *Nonlinear Dynamics*, **95**(1), (2019), 579–595.

Received 5.05.2023